



**HAL**  
open science

## Improving photosynthetic efficiency toward food security: Strategies, advances, and perspectives

Edward N Smith, Marvin van Aalst, Tiina Tosens, Ülo Niinemets, Benjamin Stich, Tomas Morosinotto, Alessandro Alboresi, Tobias Erb, Paul A Gómez-Coronado, Dimitri Tolleter, et al.

### ► To cite this version:

Edward N Smith, Marvin van Aalst, Tiina Tosens, Ülo Niinemets, Benjamin Stich, et al.. Improving photosynthetic efficiency toward food security: Strategies, advances, and perspectives. *Molecular Plant*, 2023, 16 (10), pp.1547-1563. 10.1016/j.molp.2023.08.017 . hal-04212442

**HAL Id: hal-04212442**

**<https://hal.science/hal-04212442v1>**

Submitted on 20 Sep 2023

**HAL** is a multi-disciplinary open access archive for the deposit and dissemination of scientific research documents, whether they are published or not. The documents may come from teaching and research institutions in France or abroad, or from public or private research centers.

L'archive ouverte pluridisciplinaire **HAL**, est destinée au dépôt et à la diffusion de documents scientifiques de niveau recherche, publiés ou non, émanant des établissements d'enseignement et de recherche français ou étrangers, des laboratoires publics ou privés.



Distributed under a Creative Commons Attribution - NonCommercial - NoDerivatives 4.0 International License

# Journal Pre-proof

Improving photosynthetic efficiency toward food security: Strategies, advances, and perspectives

Edward N. Smith, Marvin van Aalst, Tiina Tosens, Ülo Niinemets, Benjamin Stich, Tomas Morosinotto, Alessandro Alboresi, Tobias Erb, Paul A. Gómez-Coronado, Dimitri Tolleter, Giovanni Finazzi, Gilles Curien, Matthias Heinemann, Oliver Ebenhöf, Julian M. Hibberd, Urte Schlüter, Tianshu Sun, Andreas P.M. Weber

PII: S1674-2052(23)00252-6

DOI: <https://doi.org/10.1016/j.molp.2023.08.017>

Reference: MOLP 1595

To appear in: *MOLECULAR PLANT*

Received Date: 3 July 2023

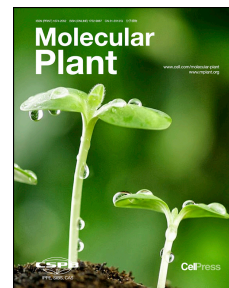
Revised Date: 20 August 2023

Accepted Date: 31 August 2023

Please cite this article as: Smith E.N., van Aalst M., Tosens T., Niinemets Ü., Stich B., Morosinotto T., Alboresi A., Erb T., Gómez-Coronado P.A., Tolleter D., Finazzi G., Curien G., Heinemann M., Ebenhöf O., Hibberd J.M., Schlüter U., Sun T., and Weber A.P.M. (2023). Improving photosynthetic efficiency toward food security: Strategies, advances, and perspectives. Mol. Plant. doi: <https://doi.org/10.1016/j.molp.2023.08.017>.

This is a PDF file of an article that has undergone enhancements after acceptance, such as the addition of a cover page and metadata, and formatting for readability, but it is not yet the definitive version of record. This version will undergo additional copyediting, typesetting and review before it is published in its final form, but we are providing this version to give early visibility of the article. Please note that, during the production process, errors may be discovered which could affect the content, and all legal disclaimers that apply to the journal pertain.

© 2023 The Author



1 **Improving photosynthetic efficiency toward food security: Strategies, advances, and**  
2 **perspectives**

3  
4 Edward N. Smith<sup>1</sup>, Marvin van Aalst<sup>2</sup>, Tiina Tosens<sup>3</sup>, Ülo Niinemets<sup>3</sup>, Benjamin Stich<sup>4\*</sup>, Tomas  
5 Morosinotto<sup>5</sup>, Alessandro Alboresi<sup>5</sup>, Tobias Erb<sup>6</sup>, Paul A. Gómez-Coronado<sup>6</sup>, Dimitri Tolleter<sup>7</sup>,  
6 Giovanni Finazzi<sup>7</sup>, Gilles Curien<sup>7</sup>, Matthias Heinemann<sup>1</sup>, Oliver Ebenhöf<sup>2</sup>, Julian M. Hibberd<sup>8</sup>,  
7 Urte Schlüter<sup>9</sup>, Tianshu Sun<sup>8</sup>, Andreas P.M. Weber<sup>9</sup>

8  
9 *Affiliations:*

10 <sup>1</sup>Faculty of Science and Engineering, Molecular Systems Biology — Groningen Biomolecular  
11 Sciences and Biotechnology, Nijenborgh 4, 9747 AG Groningen, The Netherlands

12 <sup>2</sup>Institute of Quantitative and Theoretical Biology, Cluster of Excellence on Plant Science  
13 (CEPLAS), Heinrich-Heine-University, Universitätsstrasse 1, 40225 Duesseldorf, Germany

14 <sup>3</sup>Institute of Agricultural and Environmental Sciences, Estonian University of Life Sciences, Tartu,  
15 51006 Estonia

16 <sup>4</sup>Institute of Quantitative Genetics and Genomics of Plants, Cluster of Excellence on Plant Science  
17 (CEPLAS), Heinrich-Heine-University, Universitätsstrasse 1, 40225 Duesseldorf, Germany

18 <sup>5</sup>Department of Biology, University of Padova, 35131 Padova, Italy

19 <sup>6</sup>Max Planck Institute for Terrestrial Microbiology, Department of Biochemistry & Synthetic  
20 Metabolism, 35043 Marburg, Germany

21 <sup>7</sup>Cell & Plant Physiology Laboratory, CEA-Grenoble, 38 054 Grenoble cedex 09, France

22 <sup>8</sup>Molecular Physiology, Department of Plant Sciences, University of Cambridge, Cambridge, CB2  
23 3EA, UK

24 <sup>9</sup>Institute for Plant Biochemistry, Cluster of Excellence on Plant Science (CEPLAS), Heinrich-  
25 Heine-University, Universitätsstrasse 1, 40225 Duesseldorf, Germany

26 \*current address: Institute for Breeding Research on Agricultural Crops, Federal Research Centre  
27 for Cultivated Plants, 18190 Sanitz, Germany

28  
29 *Contact:*

30 Andreas P.M. Weber

31 [aweber@hhu.de](mailto:aweber@hhu.de) +49 211 8112347

**32 Short Summary**

33

34 The role of photosynthetic energy conversion efficiency in determining solar radiation  
35 utilization for plant biomass generation is pivotal. Alongside other factors, it notably affects  
36 crop yield. We here explore opportunities to enhance crop yields through modification of  
37 photorespiration, optimizing light use, leveraging genetic variation in photosynthetic  
38 parameters for breeding, and of adopting innovative new-to-nature synthetic biology  
39 approaches.

Journal Pre-proof

**40 Abstract**

41 Photosynthesis in both crops and natural vegetation allows light energy to be converted into  
42 chemical energy, and thus forms the foundation for almost all terrestrial trophic networks on Earth.  
43 The efficiency of photosynthetic energy conversion plays a crucial role in determining the portion  
44 of incident solar radiation that can be used to generate plant biomass throughout a growth season.  
45 Consequently, alongside factors such as resource availability, crop management, crop selection,  
46 maintenance costs, and intrinsic yield potential, photosynthetic energy use efficiency significantly  
47 influences crop yield. Photosynthetic efficiency is relevant to sustainability and food security  
48 because it impacts water-use efficiency, nutrient-use efficiency, and land-use efficiency. This  
49 review focuses specifically on the potential for improvements in photosynthetic efficiency to drive  
50 a sustainable increase in crop yields. We will discuss bypassing photorespiration, enhancing light  
51 use efficiency, harnessing natural variation in photosynthetic parameters for breeding purposes,  
52 and adopting new-to-nature approaches that show promise for achieving unprecedented gains in  
53 photosynthetic efficiency.

54

**55 Keywords**

56 Photosynthesis; photorespiration; photorespiratory bypass; Natural variation; Synthetic biology;  
57 plant metabolic engineering

58

59

## 60 Introduction

61

62 Photosynthesis harnesses the energy of visible light quanta to extract electrons from water,  
63 utilizing them to convert atmospheric CO<sub>2</sub> into biomass. This crucial metabolic process originated  
64 over 2 billion years ago in an atmosphere abundant in CO<sub>2</sub> and low in oxygen. Throughout  
65 geological timescales, oxygenic photosynthesis caused a significant shift in the atmospheric O<sub>2</sub>-  
66 to-CO<sub>2</sub> ratio, resulting in a present 500-fold excess of oxygen over carbon dioxide. The enzyme  
67 responsible for CO<sub>2</sub> fixation in the Calvin-Benson cycle (CBC), known as ribulose 1,5-  
68 bisphosphate carboxylase/oxygenase (Rubisco), exhibits a higher affinity for CO<sub>2</sub> than for O<sub>2</sub>.  
69 However, under current atmospheric conditions, Rubisco frequently reacts with oxygen, leading  
70 to the production of 3-phosphoglyceric acid (3PGA) and 2-phosphoglycolic acid (2PG). Notably,  
71 2PG acts as an inhibitor for key enzymes in the CBC, namely triose phosphate isomerase and  
72 sedoheptulose 1,7-bisphosphate phosphatase (Flügel et al., 2017).

73 The two carbon atoms present in 2PG cannot be further metabolized within the CBC. Instead, the  
74 conversion of 2PG to 3PGA occurs via a metabolic pathway known as photorespiration (Bauwe,  
75 2023). During photorespiration, one out of four carbon atoms contained in two molecules of 2PG  
76 is released as CO<sub>2</sub>, *i.e.*, previously fixed carbon is lost. Additionally, the process results in the  
77 release of ammonia and the consumption of ATP and redox power. Overall, photorespiration  
78 significantly diminishes the efficiency of carbon assimilation in C<sub>3</sub> plants, leading to yield losses  
79 of approximately 30% or higher (Walker et al., 2016a). Despite its negative impact on  
80 photosynthetic efficiency, photorespiration is an essential process that enables photosynthesis in  
81 an oxygen-containing atmosphere through the breakdown of 2PG (Bauwe, 2023). Mutations  
82 affecting photorespiration are typically lethal, even in the presence of carbon concentrating  
83 mechanisms such as carboxysomes in cyanobacteria, pyrenoids in algae, or C<sub>4</sub> photosynthesis  
84 in land plants (Eisenhut et al., 2008; Zelitch et al., 2009; Levey et al., 2019). The topic of  
85 photorespiration has been extensively reviewed (Bauwe et al., 2010; Hodges et al., 2016;  
86 Eisenhut et al., 2019; Fernie and Bauwe, 2020; Bauwe, 2023; Broncano et al., 2023), rendering  
87 a detailed account of the pathway unnecessary in this work. Instead, we here focus on recent  
88 approaches aiming at mitigating the impact of photorespiration on photosynthetic efficiency.

89 To mitigate the oxygenation reaction of Rubisco, land plants have evolved carbon concentrating  
90 mechanisms, including C<sub>4</sub> and CAM photosynthesis. These pathways, however, are complex and  
91 require specific leaf anatomy. Despite significant efforts, the introduction of these photosynthetic  
92 subtypes into C<sub>3</sub> plants remains an unsolved challenge. Instead of reducing oxygenation, several  
93 research groups have focused on improving efficiency of 2PG recovery designing and

94 implementing alternative pathways that bypass photorespiration, converting 2PG into CO<sub>2</sub>,  
95 intermediates of the CBC, or metabolites of C<sub>4</sub> photosynthesis. In this review, we will explore  
96 these photorespiration bypasses and other strategies to enhance photosynthetic efficiency,  
97 considering their potential contributions to increased crop yields. Additionally, we will examine  
98 naturally occurring variations in photosynthetic efficiency and explore how such variations could  
99 be leveraged for enhancing photosynthetic efficiency through breeding. Finally, we will discuss  
100 the potential of new-to-nature pathways for increasing photosynthetic efficiency.

101

## 102 **Increasing Photosynthetic Efficiency through Photorespiratory Bypasses**

103

### 104 *Chloroplast-localized photorespiratory bypasses*

105

106 We will first describe the design and implementation of bypasses to photorespiration, focusing on  
107 *in planta* experimentally validated approaches (Figure 1). We will then discuss how such  
108 bypasses improve yield and novel strategies that have not yet been tested in plants. We will start  
109 the discussion with the designs proposed by Kebeish et al. (2007) and Maier et al. (2012) since  
110 most of the reported photorespiratory bypasses since 2012 are variations of these schemes.

111

### 112 *Intra-plastidic conversion of 2PG into 3PGA by glyoxylate carboligase and tartronate* 113 *semialdehyde reductase*

114

115 Kebeish et al. (2007) successfully introduced a bacterial glycolate metabolic pathway into the  
116 chloroplasts of *Arabidopsis thaliana*, a process that involved the incorporation of five pathway  
117 enzymes fused with chloroplast targeting peptides. The ability of certain bacteria to utilize  
118 glycolate as the sole carbon source served as the basis for this implementation. Within the  
119 bacterial glycolate pathway, glycolate dehydrogenase, composed of three subunits (GDH D, E,  
120 and F), converts glycolate to glyoxylate. Subsequently, glyoxylate carboligase (GCL) catalyzes  
121 the ligation of two glyoxylate molecules, resulting in the formation of tartronic semialdehyde and  
122 the release of one molecule of CO<sub>2</sub>. Tartronic semialdehyde is further transformed into glycerate  
123 through the action of tartronic semialdehyde reductase (TSR). Native glycerate kinase converts  
124 glycerate to 3PGA.

125

126 To establish the complete bacterial glycolate pathway, Kebeish et al. (2007) introduced the  
127 corresponding pathway components using three different plasmids. Through genetic crossings of

128 lines expressing partial pathways, they eventually combined all the components to create the full  
129 pathway. The transgenic Arabidopsis plants expressing the full pathway exhibited a two-fold  
130 increase in shoot biomass and a three-fold increase in root biomass. The transgenics also  
131 demonstrated a decrease in the glycine-to-serine ratio, which is indicative of reduced  
132 photorespiratory flux. Moreover, the post-illumination burst of CO<sub>2</sub> release, a measure of  
133 photorespiratory glycine in the light, was reduced.

134  
135 Additionally, the lines expressing the complete bacterial pathway showed a minor reduction in  
136 oxygen-inhibition of photosynthetic carbon assimilation and a slight decrease in the CO<sub>2</sub>-  
137 compensation point. These findings suggest that the implementation of the pathway resulted in a  
138 modest elevation of CO<sub>2</sub> levels at the site of Rubisco. Intriguingly, transgenic lines expressing  
139 only glycolate dehydrogenase D, E, and F also exhibited significant increases in biomass and  
140 rosette diameter, along with decreased Gly/Ser ratios. However, the reason behind the improved  
141 plant performance solely from the expression of bacterial glycolate dehydrogenase remains  
142 unexplained.

143  
144 *Intra-plastidic glycolate oxidation by glycolate oxidase*

145  
146 Maier et al. (2012) developed an alternative photorespiratory bypass strategy by redirecting  
147 peroxisomal enzymes to the chloroplasts. This pathway involves the complete oxidation of  
148 glycolate to CO<sub>2</sub> within the chloroplast stroma. To achieve this, peroxisomal glycolate oxidase  
149 was targeted to the chloroplasts, where it catalyzes the oxidation of glycolate to glyoxylate,  
150 releasing hydrogen peroxide as a byproduct. The chloroplast-targeted catalase then dissipates  
151 the hydrogen peroxide. Subsequently, glyoxylate and acetyl-CoA are condensed to malate by a  
152 plastid-targeted malate synthase, an enzyme from the peroxisomal glyoxylate cycle. Malate is  
153 decarboxylated by the native chloroplast NADP-malic enzyme, generating pyruvate and NADPH.  
154 The resulting pyruvate is further decarboxylated by the native chloroplast pyruvate  
155 dehydrogenase, yielding acetyl-CoA and NADH. Acetyl-CoA, along with another glyoxylate  
156 molecule, re-enters the cycle through malate formation via malate synthase. Overall, this cycle  
157 completely oxidizes the carbon present in glycolate and releases CO<sub>2</sub> within the chloroplast  
158 stroma. Additionally, it generates NADPH and NADH as reducing equivalents. Unlike the pathway  
159 described by Kebeish et al. (2007), the Maier et al. (2012) pathway requires the introduction of  
160 only three transgenes.

161



162 Transgenic Arabidopsis plants expressing the glycolate oxidizing pathway showed significantly  
163 increased rates of CO<sub>2</sub> assimilation and a decreased Gly/Ser ratio. However, in contrast to the  
164 findings of Kebeish et al. (2007), the CO<sub>2</sub> compensation point remained unchanged. This result  
165 is surprising considering that the local CO<sub>2</sub>/O<sub>2</sub> ratio within the chloroplasts of these lines is  
166 expected to be higher than in the lines of Kebeish et al. (2007). One of the two lines analyzed by  
167 Maier et al. (2012) exhibited increased leaf fresh and dry weight, along with a reduction in leaf  
168 thickness.

169

#### 170 *Expression of glycolate dehydrogenase in chloroplasts*

171

172 Kebeish et al. (2007) observed that transgenic Arabidopsis plants expressing all three subunits  
173 of *E. coli* glycolate dehydrogenase exhibited enhanced biomass accumulation and reduced flux  
174 through the conventional photorespiration pathway. Building upon this discovery, Nölke et al.  
175 (2014) created transgenic potato plants that were genetically modified to express a single  
176 glycolate dehydrogenase polyprotein, wherein the D, E, and F subunits were linked by a  
177 (Gly<sub>4</sub>Ser)<sub>3</sub> linker sequence. The polyprotein was targeted to the chloroplasts using a Rubisco  
178 small subunit targeting peptide (rbcS1).

179 The transgenic potato plants demonstrated elevated rates of CO<sub>2</sub> assimilation at a 400 ppm CO<sub>2</sub>  
180 concentration, decreased repression of CO<sub>2</sub> assimilation by O<sub>2</sub>, and a lowered CO<sub>2</sub> compensation  
181 point. Moreover, these transgenic lines exhibited increased above-ground biomass accumulation  
182 compared to the control plants, with a more than twofold increase in tuber yield observed in lines  
183 showing the highest glycolate dehydrogenase activity. The precise mechanism underlying the  
184 augmented biomass production and yield in the transgenic plants was not extensively investigated  
185 in this study. However, the authors put forward the hypothesis that chloroplast-produced glycolate  
186 is decarboxylated by plastidial pyruvate dehydrogenase, resulting in a localized rise in CO<sub>2</sub>  
187 concentration at the Rubisco site.

188

#### 189 *Combination of plastid-localized photorespiration bypasses with reduced export of glycolate from* 190 *chloroplasts*

191

192 South et al. (2019) conducted a comparative analysis of three alternative designs for  
193 photorespiratory bypasses (AP1-3) in tobacco, a model crop, and evaluated the performance of  
194 transgenic plants in field trials. AP1 corresponds to the pathway described by Kebeish et al.  
195 (2007), AP2 is based on the pathway reported by Maier et al. (2012), and AP3 is a modified

196 version of the Maier et al. (2012) pathway. In AP3, the combination of peroxisomal glycolate  
197 oxidase and catalase was replaced by mitochondrial glycolate dehydrogenase from *C. reinhardtii*,  
198 which was retargeted to the chloroplasts. Unlike the bacterial glycolate dehydrogenase with its  
199 three subunits, the algal mitochondrial enzyme consists of a single subunit and does not produce  
200 H<sub>2</sub>O<sub>2</sub> (the electron acceptor remains unknown), eliminating the need for co-expression of  
201 catalase. Consequently, the AP3 design only requires two transgenes: glycolate dehydrogenase  
202 and malate synthase.

203  
204 Furthermore, all three alternative pathway designs were combined with a reduction in glycolate  
205 export from chloroplasts by employing antisense repression of the chloroplastic  
206 glycolate/glycerate transporter (PLGG1, Pick et al., 2013). T2 transformants were initially  
207 screened under high light and low CO<sub>2</sub> conditions to identify lines that exhibited enhanced  
208 protection against photorespiratory stress. This pre-selection step was crucial for identifying lines  
209 with optimal expression levels and stoichiometry of the pathway components. In greenhouse  
210 trials, all pathway designs were associated with increased biomass production, with AP2 and AP3  
211 performing better when combined with repression of PLGG1. Subsequently, the AP3 design was  
212 evaluated in replicated field trials, both with and without repression of PLGG1. Surprisingly,  
213 contrary to the greenhouse experiments, the AP3 design performed best in the field without  
214 repression of PLGG1. The field-grown AP3 lines exhibited significantly higher biomass  
215 productivity, increased CO<sub>2</sub> assimilation rates, and decreased CO<sub>2</sub> compensation points.  
216 Additionally, AP3 lines displayed elevated levels of glyoxylate, while serine and glycerate levels  
217 were significantly reduced.

218  
219 This study is significant as it validated previously reported bypass designs through a comparative  
220 analysis in the same model system, demonstrating that growth benefits observed in a greenhouse  
221 setting can be reproduced in the field. However, it is worth noting that lines expressing only a  
222 chloroplast-targeted glycolate dehydrogenase from *C. reinhardtii* were not included in this  
223 comparison. This omission is a limitation as it could have provided insights into whether the  
224 improved performance observed for AP3 is truly dependent on the coordinated activity of glycolate  
225 dehydrogenase and malate synthase or if, similar to Nölke et al. (2012), glycolate dehydrogenase  
226 alone can confer growth benefits.

227  
228 *Complete oxidation of glycolate via oxalate oxidase*

229

230 The study of Shen et al. (2019) describes a modified pathway, based on the work of Maier et al.  
231 (2012), which enables complete intra-plastidic decarboxylation of glycolate. This pathway  
232 involves the conversion of glycolate to oxalate through the action of rice glycolate oxidase isoform  
233 3 (OsGLO3), previously demonstrated to oxidize both glycolate and glyoxylate (Zhang et al.,  
234 2012). The resulting oxalate is then fully decarboxylated to CO<sub>2</sub> by oxalate oxidase (OsOXO3).  
235 The accumulation of H<sub>2</sub>O<sub>2</sub>, a byproduct of glycolate and oxalate oxidation, is effectively eliminated  
236 by a chloroplast-targeted catalase. Consequently, the implementation of this pathway  
237 necessitates the incorporation of three transgenes encoding the chloroplast-targeted enzymes:  
238 glycolate oxidase, oxalate oxidase, and catalase.

239 Rice plants expressing these genetic constructs exhibited enhanced photosynthetic performance,  
240 characterized by a reduced CO<sub>2</sub> compensation point and a higher maximum photosynthetic rate  
241 under saturating light conditions. Furthermore, the Gly/Ser ratio and glycolate levels decreased,  
242 while glyoxylate and oxalate levels increased under ambient air conditions. Notably, the yield of  
243 single plant seeds varied depending on the seeding season, with a 27% increase observed in  
244 spring seeding but a yield penalty of 13-16% in fall seeding.

245 In another variation of the pathways proposed by Kebeish et al. (2007) and Maier et al. (2012),  
246 Wang et al. (2020a) substituted the bacterial glycolate dehydrogenase component of the  
247 glyoxylate carboligase route with the glycolate oxidase/catalase system in transgenic rice plants.  
248 This approach effectively combined aspects of the two previously reported bypasses. The  
249 transgenic plants exhibited improved photosynthetic parameters and yield in replicated field trials,  
250 further confirming the potential of photorespiratory bypasses to enhance crop performance under  
251 field conditions.

252

### 253 *Peroxisome-localized photorespiratory bypasses*

254

255 In the native photorespiration process, glycolate is transported from chloroplasts to peroxisomes.  
256 Within the peroxisomes, glycolate undergoes oxidation by glycolate oxidase, resulting in the  
257 production of glyoxylate. Subsequently, glyoxylate is transaminated to form glycine. The glycine  
258 molecules are then transported to the mitochondria, where glycine decarboxylase and serine  
259 hydroxymethyltransferase catalyze the conversion of two glycine molecules into serine, CO<sub>2</sub>, and  
260 ammonia. The generated serine is subsequently transported back to the peroxisomes, where it is  
261 converted into hydroxypyruvate by the action of serine:glyoxylate aminotransferase.  
262 Hydroxypyruvate is further reduced to glycerate, which is then transported back to the  
263 chloroplasts, thereby completing the photorespiratory cycle. Given the crucial role of peroxisomes

264 in photorespiration, researchers have endeavored to develop strategies for bypassing the  
265 ammonia and CO<sub>2</sub>-releasing step that occurs in the mitochondria, through alternate glycolate  
266 conversion within peroxisomes. Two such attempts have been documented in the literature.

267

#### 268 *Peroxisomal conversion of glyoxylate to hydroxypyruvate*

269

270 This pathway design capitalizes on the conversion of glycolate to glyoxylate by the inherent  
271 peroxisomal glycolate oxidase, aiming to redirect glyoxylate towards hydroxypyruvate through the  
272 involvement of glyoxylate carboligase and hydroxypyruvate isomerase. Similar to the pathway  
273 design proposed by Kebeish et al. (2007), bacterial glyoxylate carboligase is employed to convert  
274 glyoxylate into tartronate semialdehyde, which is subsequently transformed into hydroxypyruvate  
275 by hydroxypyruvate isomerase. Essentially, this strategy enables the retrieval of 75% of the  
276 carbon content present in two glyoxylate molecules, while mitigating the release of ammonia  
277 mediated by mitochondrial glycine decarboxylase. Transgenic tobacco plants carrying constructs  
278 encoding peroxisome-targeted versions of these bacterial enzymes were generated.

279 Under non-photorespiratory conditions at high-CO<sub>2</sub>, the transgenic plants exhibited robust growth.  
280 However, when exposed to current ambient CO<sub>2</sub> conditions, the leaves displayed yellow lesions,  
281 and the plants exhibited a chlorotic phenotype. Metabolic labeling experiments employing [<sup>14</sup>C]-  
282 glycolate revealed that glycolate was still predominantly converted into glycine and subsequently  
283 serine, suggesting that only a minor fraction of glycolate entered the engineered pathway.  
284 Surprisingly, amino acid analysis indicated that the leaves of the transgenic plants contained  
285 higher levels of glycine and serine compared to wild-type plants, contrary to initial expectations.  
286 Notably, the researchers were unable to detect the presence of the hydroxypyruvate isomerase  
287 protein in the transgenic plants through immunoblotting, despite the detectable expression of the  
288 transgene confirmed by RNA gel blots. These findings suggest that the pathway may have been  
289 incomplete, and the observed phenotypes could arise from the accumulation of undesired  
290 tartronate semialdehyde in peroxisomes, exerting adverse effects.

291

#### 292 *Peroxisomal glyoxylate to oxaloacetate conversion via the beta-hydroxyaspartate shunt*

293

294 In this study (Roell et al., 2021), a recently discovered microbial pathway involved in the  
295 metabolism of glyoxylate was introduced into plant peroxisomes. The pathway, known as the  $\beta$ -  
296 hydroxyaspartate cycle, encompasses four enzymatic steps that convert glyoxylate and glycine  
297 into oxaloacetate. The sequential actions of  $\beta$ -hydroxyaspartate aldolase,  $\beta$ -hydroxyaspartate

298 dehydratase, and iminosuccinate reductase transform glyoxylate and glycine into  $\beta$ -  
299 hydroxyaspartate, iminosuccinate, and aspartate, respectively. Finally, aspartate:glyoxylate  
300 aminotransferase converts glyoxylate into glycine, and releases oxaloacetate as the end product  
301 of the pathway. Transgenic Arabidopsis plants were engineered to express the pathway enzymes  
302 fused with peroxisomal targeting signals. Promoters that drive gene expression specifically in  
303 photosynthetic tissues were employed to prevent undesired pathway activity in non-  
304 photosynthetic plant organs.

305 Roell et al. (2021) hypothesized that reducing the conversion of glyoxylate to glycine would  
306 enhance metabolic flux through the  $\beta$ -hydroxyaspartate cycle. Therefore, apart from wild-type  
307 Arabidopsis plants, the pathway was introduced into the genetic background of the *ggt1-1* mutant,  
308 which lacks peroxisomal glutamate:glyoxylate aminotransferase 1 and exhibits a photorespiratory  
309 phenotype under ambient air conditions. This enabled the investigation of the  $\beta$ -hydroxyaspartate  
310 cycle's function by assessing its ability to complement the visual phenotype of the *ggt1-1* mutant.  
311 Similar to the findings of Carvalho et al. (2011), wild-type plants expressing the  $\beta$ -  
312 hydroxyaspartate cycle exhibited reduced growth and photosynthetic rates in ambient air.  
313 However, when exposed to elevated CO<sub>2</sub> concentrations that suppress photorespiration, their  
314 growth was comparable to that of wild-type controls. Importantly, the expression of the  $\beta$ -  
315 hydroxyaspartate cycle in the *ggt1-1* mutant partially rescued the photorespiratory phenotype,  
316 indicating that the introduced pathway fulfilled its expected function to some extent.

317 Metabolic analysis was conducted to investigate the underlying reasons for the impaired growth  
318 observed in wild-type transgenic plants expressing the  $\beta$ -hydroxyaspartate cycle. These plants,  
319 as well as the transformed *ggt1-1* mutants, exhibited elevated levels of aspartate and malate,  
320 while glycine levels were reduced. Furthermore, intermediates of the CBC, such as 3-  
321 phosphoglycerate and sedoheptulose 7-phosphate, were depleted, suggesting a decrease in the  
322 availability of CBC intermediates and unproductive metabolic flux into C<sub>4</sub> acids.

323  
324 Collectively, the studies by Carvalho et al. (2011) and Roell et al. (2021) indicate that perturbing  
325 the peroxisomal steps of the canonical photorespiration pathway does not yield the anticipated  
326 improvement in photosynthetic performance.

327  
328 Although not extensively discussed in this review, we note that bypasses to photorespiration often  
329 led to a multitude of pleiotropic changes, including alterations in leaf shape and anatomy,  
330 metabolic changes, and developmental effects. For example, changes in leaf anatomy can have  
331 a multitude of effects on leaf photosynthetic activities. Changes in leaf thickness alone can result

332 in increased photosynthetic activity due to more photosynthetic biomass per unit leaf area (Onoda  
333 et al., 2017). Changes in leaf anatomy such as modifications in leaf thickness, intercellular  
334 airspace volume, mesophyll cell wall thickness and chloroplast size can also affect mesophyll  
335 conductance for CO<sub>2</sub> ( $g_m$ , see Figure 2 for a schematic explanation of  $g_m$ ), and thereby alter the  
336 CO<sub>2</sub> concentration in chloroplasts (Flexas et al., 2012; Flexas et al., 2013; Knauer et al., 2022).  
337 Given that observed changes in the CO<sub>2</sub> compensation points have often been small in the above-  
338 mentioned studies, consideration of possible changes in  $g_m$  is important. We also note that the  
339 CO<sub>2</sub> compensation point does not only depend on Rubisco characteristics and CO<sub>2</sub> and O<sub>2</sub>  
340 concentrations, but is also affected by the rate of mitochondrial respiration in light ( $R_d$ ).  $R_d$  may  
341 change as a consequence of pathway engineering, for example, generation of extra respiratory  
342 substrate such as malate transported out of chloroplasts.

343 The precise relationship between modified photorespiration and its impact on plant structure and  
344 function, beyond photosynthesis, remains incompletely understood. It is important to  
345 acknowledge that native photorespiration does not operate as a closed cycle in which 75% of the  
346 carbon derived from glycolate is reincorporated into the CBC as glycerate and 25% are released  
347 as CO<sub>2</sub>. Instead, considerable amounts of carbon can be diverted towards the synthesis of amino  
348 acids glycine and serine (Samuilov et al., 2018; Abadie and Tcherkez, 2019; Fu et al., 2023a),  
349 which serve as building blocks for protein biosynthesis and other plant metabolites. Moreover,  
350 photorespiration indirectly transfers redox equivalents from chloroplasts to mitochondria (Heber  
351 and Krause, 1980; Heber et al., 1996), where they are oxidized by the mitochondrial electron  
352 transport chain, contributing to ATP biosynthesis. The observed effects extending beyond  
353 photosynthetic metabolism may be linked to these additional, albeit less extensively studied and  
354 recognized, functions of the photorespiratory pathway. In the following paragraphs, we will provide  
355 a critical assessment of the assumptions as to how photorespiratory bypasses function and we  
356 highlight unresolved questions on these pathways.

357

### 358 *A critical qualitative assessment of mechanistic hypotheses*

359

360 Despite the fact that some of the genetic implementations of photorespiratory bypasses increased  
361 photosynthetic efficiency and even yield under some conditions, many questions remain  
362 unresolved. In particular the precise molecular mechanisms that are responsible for higher  
363 performance are not yet understood. In order to develop informed hypotheses which are also  
364 backed up by theoretical considerations, we give some qualitative and quantitative arguments  
365 about attempts to explain increased photosynthetic rates.

366 First, it should be noted that an observation of biomass increases of a certain percentage after a  
367 - usually several weeks long - growth period, cannot be directly translated into increased fluxes.  
368 Even marginal differences in flux will, over time, lead to an exponential difference in overall  
369 biomass accumulation. For example, in South et al. (2019) it was shown that under saturating  
370 CO<sub>2</sub> the assimilation rate is increased by approximately 10% (cf. South et al., 2019, Fig. 5A).  
371 However, this increase is considerably lower than the reported 24% increase in biomass after a  
372 growth period of 6 weeks. This example illustrates that yield gains in percent stated for the diverse  
373 experimental approaches are not comparable on a quantitative level.

374 Other observations in South et al. (2019) are also challenging to explain. For example, it has been  
375 suggested that an increase in CO<sub>2</sub> *locally* in the chloroplast could explain a higher carbon fixation  
376 rate. However, an increased CO<sub>2</sub> assimilation was observed even for saturating conditions, which  
377 entails that increasing the local concentration is not the primary cause for higher fixation rates. A  
378 similar result was observed when a complete glycolate decarboxylation pathway was expressed  
379 in rice with several transgenic lines showing increased maximum rates of Rubisco carboxylation  
380 under saturating CO<sub>2</sub> (Shen et al., 2019). Another hypothesis was that as a result of the glycolate  
381 oxidase activity, glycolate levels should be reduced, and thus reducing its toxic effects. However,  
382 in various lines the glycolate levels were actually increased, making also this explanation unlikely.  
383 Similarly, although not explicitly measured, 2PG levels might be reduced as a result of the newly  
384 introduced pathways, but because the dephosphorylation of 2PG to glycolate is highly irreversible,  
385 there is no convincing argument why 2PG levels should actually be reduced. We note, however,  
386 that it was previously shown that more efficient removal of 2PG by over-expression of 2-  
387 phosphoglycolate phosphatase improved photosynthetic performance in *Arabidopsis thaliana*  
388 under stress conditions (Timm et al., 2019).

389 Possibly, the growth promoting effect is of a more indirect nature. A possible explanation could  
390 be connected with the algal glycolate dehydrogenase, which transfers electrons not to H<sub>2</sub>O<sub>2</sub> but  
391 to a so far unidentified electron acceptor. If this acceptor is one of the common electron carriers  
392 of the photosynthetic electron transport chain, such as plastoquinone or ferredoxin, then this new  
393 pathway would contribute to the generation of redox equivalents and thus directly support the  
394 photosynthetic electron transport chain. The observation that the transformed plants exhibit a  
395 higher apparent quantum efficiency ( $\phi$ , cf. South et al., 2019, Fig. 6) is in line with this hypothesis.  
396 An experimental test would be to measure how the observed increase in growth depends on the  
397 light intensity under which plants are grown. If this speculation is correct, the growth increase  
398 should be less pronounced the more saturating the light intensity.

399 In summary, these considerations illustrate the complexity of the system and the necessity to use  
400 mathematical models, which are based on clear mechanistic hypotheses and are designed to  
401 quantitatively reproduce experimental results and thus provide a platform to test different  
402 mechanistic hypotheses and, by making novel predictions, support the experimental design to  
403 confirm or falsify these.

404

#### 405 *Modeling at different scales can inform photorespiration engineering*

406

407 The mechanisms of yield improvement caused by photorespiratory bypasses can be divided into  
408 four categories: improved stoichiometry and energy efficiency, improved kinetics (*i.e.*, altered  
409 Rubisco carboxylation-to-oxygenation ratio), relief of inhibition by toxic intermediates, and indirect  
410 effects of altered physiology or development. Models at different scales, from simple cofactor  
411 accounting and stoichiometric models, to kinetic models of photosynthesis, have provided some  
412 insight into how these mechanisms allow photorespiratory bypasses to be effective but further  
413 work is still required if models are to explain all observed experimental results (Peterhansel et al.,  
414 2013; Xin et al., 2015; Basler et al., 2016; Trudeau et al., 2018; Khurshid et al., 2020; Osmanoglu  
415 et al., 2021).

416 A common feature of photorespiratory bypasses is to avoid the energetic cost of ammonium  
417 refixation or to capture the reducing power from glycolate oxidation, thus decreasing the ATP and  
418 NADPH cost of photorespiration. Models for energy cofactor accounting can quantify these direct  
419 energetic benefits of bypassing photorespiration, as well as indirect benefits such as avoiding the  
420 cost of CO<sub>2</sub> refixation via the CBC in carbon fixing bypasses (Table 1) (Peterhansel et al., 2013;  
421 Trudeau et al., 2018). Larger, genome scale stoichiometric models can also calculate energy  
422 efficiency and have the advantage of predicting flux into biomass rather than just rates of carbon  
423 fixation, placing bypasses in the wider context of the plant metabolic network (Basler et al., 2016).  
424 For example, a curated stoichiometric model was able to predict a decrease in photorespiratory  
425 flux and a biomass output increase of ~6.2%, qualitatively consistent with experimental data  
426 (Basler et al., 2016; Kebeish et al., 2007). However, stoichiometric models predict no benefit for  
427 bypasses that are energetically more costly than photorespiration, such as those that completely  
428 decarboxylate glycolate in the chloroplast. Experimentally, such bypasses still show increased  
429 yields when expressed in plants, suggesting either incorrect prediction of energy costs, or benefits  
430 that are beyond just direct ATP and NADPH savings (Maier et al., 2012; Peterhansel et al., 2013;  
431 Shen et al., 2019; South et al., 2019; Xin et al., 2015).



432 Photorespiration involves the transport of metabolites between three compartments, as well as  
433 the movement of reducing equivalents from the chloroplasts to the mitochondria. Photorespiratory  
434 bypasses can relocate reactions to different compartments, potentially avoiding the energetic  
435 costs of metabolite transport. Therefore, more complete modeling of transport reactions, including  
436 thermodynamic constraints may improve the accuracy of energy accounting. However, even if  
437 all energetic costs were accurately modeled, stoichiometric models alone cannot account for  
438 changes in metabolite concentrations or reaction kinetics.

439 Several of the bypasses validated in plants aim to relocate the release of photorespiratory CO<sub>2</sub>  
440 from the mitochondria to the chloroplasts which has two potential advantages: increasing the CO<sub>2</sub>  
441 concentration at the site of Rubisco, and recapturing photorespiratory CO<sub>2</sub> that could otherwise  
442 be lost from the cell by diffusion out of mitochondria. Predicting such effects requires the use of  
443 kinetic models or additional constraints on Rubisco carboxylation and oxygenation fluxes (Basler  
444 et al., 2016). A kinetic model predicted that under high light conditions, the entire benefit of the  
445 Kebeish et al., (2007) bypass is the relocation of CO<sub>2</sub> release, not the reduced ATP cost, which  
446 only contributes under low light conditions (Xin et al., 2015). However, the same kinetic model  
447 failed to explain the benefit of complete glycolate decarboxylation in the chloroplast, predicting  
448 that photosynthetic rate would be 31% lower than in the wild-type, despite reported increases of  
449 >30% in carbon assimilation rate and biomass (Maier et al., 2012; Xin et al., 2015). Additionally,  
450 the kinetic model demonstrated that any benefit of relocating CO<sub>2</sub> release is dependent on the  
451 CO<sub>2</sub> permeability of the chloroplasts; predicting that if >30% of photorespired CO<sub>2</sub> is already  
452 recaptured and refixed in wild-type plants, then there is no benefit to the bypass (Xin et al., 2015).  
453 It is therefore surprising that a glycolate decarboxylation bypass in rice, where wild-type plants  
454 already refix 38% of photorespiratory CO<sub>2</sub>, still showed some biomass gains, suggesting  
455 additional benefits not captured by the kinetic model (Busch et al., 2013; Xin et al., 2015; Shen et  
456 al., 2019; Wang et al., 2020a; Zhang et al., 2022).

457 In contrast to Xin et al. (2015), a different kinetic model of a cyanobacterial complete glycolate  
458 decarboxylation bypass expressed in the chloroplast predicted a 10% increase in photosynthetic  
459 rate, although this model did not explicitly account for the movement of CO<sub>2</sub> between  
460 compartments and is yet to be experimentally validated by expression of the full pathway in plants  
461 (Bilal et al., 2019; Khurshid et al., 2020; Abbasi et al., 2021). Kinetic models have therefore been  
462 useful for estimating the potential effect of relocation of CO<sub>2</sub> release and distinguishing this from  
463 energy benefits, but they are still unable to explain all currently observed experimental results.

464 Reducing the concentration of inhibitory intermediates of photosynthetic metabolism could  
465 account for some of the benefit of photorespiratory bypasses, and this can be simulated using

466 kinetic models. However, kinetic models of photorespiratory bypasses did not include parameters  
467 for the inhibitory effects of 2-phosphoglycolate on the CBC or the inhibitory effect of glyoxylate on  
468 Rubisco activation and Rubisco oxygenase activity (Oliver and Zelitch, 1977; Oliver, 1980;  
469 Campbell and Ogren, 1990; Xin et al., 2015; Flügel et al., 2017; Khurshid et al., 2020). Increasing  
470 the scale of kinetic models to include more inhibition terms may provide additional explanation for  
471 benefits, although this can be limited by the availability of accurate kinetic parameters.

472 As pointed out previously, a higher apparent quantum efficiency could be responsible for yield  
473 improvements in the transformed plants. Modeling the effect of bypasses on quantum efficiency  
474 would require a high-fidelity kinetic model of the photosynthetic electron transport chain and the  
475 CBC, such as Saadat et al. (2021), to be combined with a model of photorespiration.

476 Additional effects beyond the cellular metabolic changes described by current models such as  
477 altered gene expression, signaling, physiology, and pleiotropic effects could also explain a large  
478 proportion of observed growth benefits (Maier et al., 2012; Shen et al., 2019). Using larger scale  
479 integrated models could potentially provide more accurate prediction of the effect of engineering  
480 photorespiration in the field by accounting for interactions across scales (Wu, 2023). Additionally,  
481 attempting to model dynamic processes under non-steady state conditions may also help identify  
482 advantages of photorespiratory bypasses not captured by current models (Fu et al., 2023b).  
483 Finally, extending current metabolic models to account for diurnal cycles could explain  
484 advantages of bypass reactions beyond altered photosynthetic metabolism, such as altered dark  
485 respiration and sucrose export during the night (Dalal et al., 2015).

486 No single modeling strategy can explain all of the observed phenotypes of plants expressing  
487 photorespiratory bypasses and instead multiple models at different scales should be used as tools  
488 to help explain the underlying mechanisms of growth benefits. Questions still remain to be tested  
489 by exploring models: why does expression of glycolate dehydrogenase alone also increase  
490 photosynthetic performance and yield in Arabidopsis, potato, and Camelina (Abbasi et al., 2021;  
491 Dalal et al., 2015; Kebeish et al., 2007; Nölke et al., 2014); and how does the anatomy and  
492 physiology of different crop species affect CO<sub>2</sub> diffusion between cells and subcellular  
493 compartments? Future implementation of new bypass designs based on carbon fixing, rather than  
494 decarboxylating, reactions will also provide valuable data for exploring the effect of a  
495 fundamentally different bypass mechanism (Trudeau et al., 2018; Scheffen et al., 2021) (see  
496 discussion of *new-to-nature pathways* below). With future modeling efforts and better  
497 understanding, it may be possible to further increase yields and improve the transferability of  
498 benefits between different crop species.

499

Journal Pre-proof

501 **Table 1.** Photorespiratory bypass energy costs (adapted from Trudeau et al., 2018). Based on  
 502 the consumer model of photosynthesis which describes the processes of photorespiration and  
 503 the Calvin-Benson cycle as independent cycles that are able to regenerate ribulose 1,5-  
 504 biphosphate using ATP ( $\beta$ ) and reducing equivalents ( $\gamma$ ) and either consume or produce  $\text{CO}_2$   
 505 and glyceraldehyde 3-phosphate (GAP) ( $\alpha$ ) (Trudeau et al., 2018). This description allows  
 506 bypasses to be compared directly and separated from the Calvin-Benson cycle. Positive values  
 507 represent consumption, negative values represent production. See supplementary table 1 for  
 508 detailed calculations. \*3OHP bypass assuming pyruvate is converted to GAP via pyruvate  
 509 phosphate dikinase. \*\*BHAC bypass assuming oxaloacetate is converted to GAP via  
 510 phosphoenolpyruvate-carboxykinase in order to regenerate RuBP. † assuming 2.5 ATP per  
 511 reducing equivalent. †† assuming Calvin-Benson cycle compensates for carbon lost by PR  
 512 bypasses.

513

Reference	Pathway name	$\text{CO}_2$ ( $\alpha$ )	ATP ( $\beta$ )	Red. equiv. ( $\gamma$ )	Total ATP equiv.†	Total ATP equiv.† normalised to net 0 carbon lost/gained††
Trudeau et al., 2018	TaCo	1	7	4	17	9
Kebeish et al., 2007	Chloroplast TSS	-0.5	3	1	5.5	9.5
Shih et al., 2014	3OHP*	1	8	4	18	10
Carvalho et al., 2011	Peroxisome TSS	-0.5	3	2	8	12
Roell et al., 2021	BHAC**	-0.5	3	2	8	12
	Photorespiration	-0.5	3.5	2	8.5	12.5
South et al., 2019	AP3	-2	2	-2	-3	13
Maier et al., 2012	GMK	-2	2	-1	-0.5	15.5
Shen et al., 2019	GOC	-2	2	1	4.5	20.5
	Calvin cycle	1	3	2	8	

514

515 *Abbreviations: 3OHP, 3-hydroxypropionate; Red equiv, reducing equivalents; TaCo, tartronyl-CoA; TSS, tartronic-*  
 516 *semialdehyde shunt; BHAC, beta-hydroxyaspartate cycle; GMK, glycolate oxidase, malate synthase, catalase (KatE);*  
 517 *AP3, alternative pathway 3; GOC, glycolate oxidase, oxalate oxidase, catalase.*

518

519

520

**521 Combined Optimization of Light Use and Carbon Assimilation Efficiency to Enhance Plant**  
**522 Productivity**

523

524 The intricate relationship between light conversion, carbon fixation, and their impact on plant  
525 productivity calls for a comprehensive exploration of their interdependencies. Through combining  
526 modifications to light utilization and carbon fixation, we have the potential to achieve synergistic  
527 enhancements. We here discuss the interplay between these pathways and evaluate the  
528 possibility of maximizing overall productivity by improving the efficiency of converting light energy  
529 into ATP and NADPH while optimizing their utilization for carbon fixation.

530

531 In plants, pigments absorb light, and the excitation energy is utilized by photosystems to facilitate  
532 the synthesis of ATP and NADPH, which are essential for all metabolic reactions, including carbon  
533 fixation. This initial phase of photosynthetic reactions effectively transforms light into chemical  
534 energy, and its efficiency significantly influences crop productivity (Zhu et al., 2010).

535 In highly dynamic environments, the amount of light absorbed by the photosynthetic apparatus  
536 can exceed the metabolic capacity of the cell, resulting in the over-reduction of the photosynthetic  
537 electron transport chain and the production of harmful reactive oxygen species (ROS).  
538 Photosynthetic organisms have evolved various mechanisms to regulate light utilization efficiency  
539 and photosynthetic electron transport, aiming to minimize the likelihood of over-reduction and  
540 cellular damage by safely dissipating excess excitation or electrons (Li et al., 2009). While the  
541 protection of the photosynthetic apparatus plays a crucial biological role, it comes at the expense  
542 of reduced efficiency in converting sunlight into chemical energy (Alboresi et al., 2019).

543 Fluctuations in light intensity represent a particular challenge to the regulation of photosynthesis  
544 and significantly impact primary productivity (Long et al., 2022). Abrupt increases in illumination  
545 can be detrimental as they do not allow sufficient time for the activation of regulatory responses  
546 and modulation of metabolic reactions. Conversely, when light levels decrease from excessive to  
547 limiting, the photoprotective mode remains active for several minutes, leading to unnecessary  
548 energy dissipation and a subsequent reduction in carbon fixation efficiency (Wang et al., 2020b).

549

550 To address this limitation, modifications were made to the kinetics of Non-Photochemical  
551 Quenching (NPQ), which is one of the mechanisms involved in light harvesting regulation. By  
552 overexpressing key proteins such as PsbS, VDE, and ZEP, the activation and relaxation kinetics  
553 of NPQ were accelerated. This overexpression allowed tobacco and soybean plants to effectively

554 respond to changes in light and minimize potential damage during sudden increases in sunlight.  
555 Additionally, it facilitated faster relaxation of NPQ when illumination intensity decreased. This  
556 approach has demonstrated positive effects on biomass productivity not only in the field for crops  
557 like tobacco and soybean (Kromdijk et al., 2016; Souza et al., 2022), but also in high-density  
558 culture photobioreactors for the microalga *Nannochloropsis* (Perin et al., 2023). However, in  
559 *Arabidopsis*, the same approach was not as successful, suggesting that species-specific traits,  
560 including light distribution within the canopy, significantly impact plant productivity and the optimal  
561 balance between light harvesting and photoprotective responses (Garcia-Molina and Leister,  
562 2020).

563 Another strategy to enhance the efficiency of sunlight utilization is the modification of the light  
564 harvesting apparatus. Leaves have evolved to efficiently capture light and outcompete other  
565 organisms for sunlight. However, in densely cultivated fields, this high light harvesting efficiency  
566 can have negative consequences. Light is primarily absorbed by the uppermost leaves in the  
567 canopy, leaving fewer photons available for the lower layers. While high light harvesting efficiency  
568 provides a competitive advantage in natural environments where individuals vie for a limited  
569 resource like light, it proves detrimental in cultivated fields. In this context, plants with paler leaves  
570 can enable a more uniform distribution of light within the canopy, which has been shown to  
571 enhance overall productivity (Rotasperti et al., 2022; Cutolo et al., 2023). Also, extra nitrogen that  
572 is no longer needed for construction of pigment-binding machinery of photosynthesis, could be  
573 invested in Rubisco and rate-limiting proteins of photosynthetic machinery, thereby increasing  
574 leaf photosynthetic capacity (Walker et al., 2017; Niinemets, 2023). It is interesting here to discuss  
575 if these efforts in modulating regulation of light harvesting could be combined with improvements  
576 in carbon fixation efficiency. In principle, a higher efficiency conversion of light energy into ATP  
577 and NADPH could be combined with a more efficient utilization of these molecules for carbon  
578 fixation, with a potentially additive effect on productivity.

579 One possible implication to be considered is that photorespiration has been shown to be a major  
580 sink for photosynthetic electron transport, and that this energy loss can have a beneficial effect in  
581 conditions where photosynthetic apparatus is over-excited (Heber and Krause, 1980; Kozaki and  
582 Takeba, 1996; Hanawa et al., 2017). Light saturation occurs when electron transport is faster than  
583 the metabolic capacity of consuming ATP and NADPH produced and, in these conditions,  
584 photorespiration can be beneficial in reducing over-saturation. If efficiency in carbon fixation is  
585 improved by introduction of photorespiratory bypasses, however, this would also drive to a  
586 stronger ATP and NADPH consumption with a similar protecting effect. This suggests that the  
587 critical point is that the new or modified pathways have a sufficient capacity to compensate also

588 for ATP and NADPH consumption associated with photorespiration. If this is the case their  
589 introduction will increase CO<sub>2</sub> fixation while also complementing the role of photorespiration in  
590 protection from light excess.

591 It is anticipated that altering crucial pathways in plant metabolism, including light conversion and  
592 carbon fixation, will inherently possess interdependent effects that require additional investigation.  
593 Furthermore, there exists the possibility of enhancing the efficiency of converting light energy into  
594 ATP and NADPH, while concurrently optimizing the utilization of these molecules for carbon  
595 fixation. Such combined improvements could potentially yield an additive outcome, thereby  
596 maximizing the overall impact on productivity.

597

### 598 **Leveraging Naturally Occurring Variation in Photosynthetic Parameters**

599

600 *Exploiting the natural variation of Rubisco kinetic traits,  $\Gamma^*$ , and photorespiration in coordination*  
601 *with CO<sub>2</sub> diffusion*

602

603 Leveraging the inherent diversity in essential photosynthetic traits presents two notable  
604 advantages: first, it provides engineering with essential knowledge about potential trade-offs, and  
605 secondly, it facilitates the breeding process, allowing for accelerated improvements in crops. The  
606 crucial traits related to photorespiration in Rubisco include the Michaelis-Menten constant for CO<sub>2</sub>  
607 ( $K_c$ ), the Michaelis-Menten constant for O<sub>2</sub> ( $K_o$ ), and Rubisco specificity to CO<sub>2</sub> over O<sub>2</sub> ( $S_{c/o}$ ), and  
608 maximum turnover rates (specific activity per active center per mass or protein, s<sup>-1</sup>) for  
609 carboxylase ( $V_c$ ) and oxygenase ( $V_o$ ). Several authors have investigated the environmental and  
610 evolutionary trends of natural variation in Rubisco's kinetic properties and their temperature  
611 responses, including several recent meta-analyses (Galmés et al., 2019; Bouvier et al., 2021;  
612 Tcherkez and Farquhar, 2021). These studies have revealed substantial variability in major kinetic  
613 traits, which are highly sensitive to factors such as temperature, CO<sub>2</sub> availability, and  
614 photosynthetically active quantum flux density. Moreover, this variability is inherent among  
615 species adapted to different environments. There are several key trade-offs among Rubisco  
616 kinetic traits, most notably the reverse relationships between  $S_{c/o}$  and  $V_c$  (Galmes et al. 2014,  
617 2019), which are important to consider in Rubisco engineering.

618 Recent findings have demonstrated a strong co-regulation between the natural diversity of  
619 Rubisco kinetics and mesophyll conductance ( $g_m$ ) as well as in underlying anatomical traits. For  
620 instance, plants adapted to drought exhibit reduced  $g_m$  and chloroplast CO<sub>2</sub> concentration ( $C_c$ )  
621 due to higher mesophyll cell wall thickness. Consequently, these plants possess Rubisco with

622 higher  $S_{c/o}$  but lower turnover rates (Galmés et al., 2019). This highlights the substantial influence  
623 of the  $C_c$  associated with species adaptation on the diversity of Rubisco's kinetic properties and  
624 the trade-offs observed. Importantly, this regulation is significantly influenced by  $g_m$ , which exhibits  
625 considerable variation among species and is responsive to environmental stressors. (Elferjani et  
626 al. 2020; Knauer et al. 2022)

627 It is noteworthy that  $g_m$  can limit photosynthesis, accounting for approximately 10-70% of the  
628 limitation, thereby exerting an equally significant impact on photosynthetic assimilation ( $A$ ) as  
629 stomatal conductance ( $g_s$ ) does (Knauer et al., 2020).

630 The  $CO_2$  compensation point ( $\Gamma$ ) has traditionally served as a parameter reflecting Rubisco  
631 functionality and photosynthetic efficiency. It represents the equilibrium between the  $A$  and leaf  
632 respiration, making it a useful characteristic for categorizing crops and herbaceous species based  
633 on their inherent photosynthetic efficiency and stress resilience. In  $C_3$  plants,  $\Gamma$  is typically highest  
634 (40 - 100  $\mu\text{mol mol}^{-1}$ ), intermediate in  $C_3$ - $C_4$  intermediates (20 - 30  $\mu\text{mol mol}^{-1}$ ), and low in  $C_4$   
635 plants (3 - 10  $\mu\text{mol mol}^{-1}$ ) (Nobel, 1991; Schlüter et al., 2023).

636 However,  $\Gamma$  is a complex trait and can be estimated in a multitude of ways. To incorporate Rubisco  
637 kinetics, photorespiration, and more accurately, an alternative parameter called the  
638 photorespiratory  $CO_2$  compensation point in absence of day respiration ( $\Gamma^*$ ) has been proposed.  
639  $\Gamma^*$  can be determined from  $A/C_c$  curves by using the common interception method measured at  
640 different light intensities, and represents the  $C_c$  at which photosynthetic carbon uptake equals  
641 photorespiratory  $CO_2$  release (Walker et al., 2016b).  $\Gamma^*$  and  $\Gamma$  differ significantly, the magnitude  
642 of difference depends on the variable  $g_m$  (Figure 2) and the fate of the mitochondrial  $CO_2$  fluxes,  
643 as both estimates affect the resulting  $C_c$  and  $\Gamma^*$ . The understanding of partitioning of respiratory  
644 fluxes between the proportion directed into the chloroplast and what diffuses into the cytoplasm  
645 and intercellular airspace is also crucial for correct  $g_m$  estimations. However, the fate of  
646 respiratory fluxes and  $g_m$  largely depend on similar anatomical traits, such as the proportion of  
647 mesophyll cell surface area lined with chloroplasts, and physical dimensions of cell wall,  
648 chloroplasts, and cytoplasm (Figure 2B). All these traits vary significantly across species referring  
649 to substantial variability in partitioning of respiratory fluxes between the chloroplasts and  
650 cytoplasm (von Caemmerer et al., 1994; Tosens et al., 2012; Ubierna et al., 2019). Thus,  
651 considering the physiological nature of  $CO_2$  compensation points estimated through different  
652 methods, including  $\Gamma^*$ , offers valuable insights into how mitochondrial  $CO_2$  effluxes curb  $C_c$   
653 (Walker et al., 2016b; Busch, 2020; Sage et al. 2022).

654



655

656 Achieving optimal photosynthetic efficiency requires precise coordination between traits that  
657 regulate CO<sub>2</sub> diffusion efficiency and the functionality of Rubisco. Consequently, a major focus  
658 in improving photosynthesis, whether through breeding or engineering, is to explore and  
659 comprehend the natural diversity of key kinetic traits of Rubisco and their relationship with CO<sub>2</sub>  
660 availability in the chloroplast stroma (Walker et al., 2016b; Galmés et al., 2019; Flexas and  
661 Carriquí, 2020; Evans, 2021; Knauer et al., 2022; Iqbal et al., 2023). In angiosperms with  
662 elevated rates of turnover, the constraints of photosynthesis, including stomata, mesophyll  
663 conductance, and photo/biochemical processes, typically coexist in a harmonious equilibrium,  
664 unless stress-induced alterations disrupt this balance. Consequently, attaining optimal  
665 enhancements in photosynthesis and resource utilization efficiency requires the simultaneous  
666 manipulation of all three constraints or a shift in focus towards augmenting the  $g_m/g_s$  ratio. This  
667 approach enables a simultaneous increase in intrinsic water-use efficiency (Gago et al., 2019;  
668 Flexas and Carriquí, 2020; Knauer et al., 2020; Clarke et al., 2022; Kromdijk and McCormick,  
669 2022).

670

671 Previous studies have often addressed the kinetic components of  $A/C_i$  curves (Rubisco kinetics,  
672 RuBP turnover rate, electron transport limitations;  $R_d$ , respiration due to photorespiration [ $R_p$ ],  
673 CO<sub>2</sub> compensation point) separately, combining *in vivo* and *in vitro* estimations, resulting in  
674 fragmented information (Bernacchi et al., 2013). However, employing state-of-the-art fast  
675 response gas-exchange and optical diagnostic systems, as described by Laisk et al. (2002),  
676 allows for the simultaneous measurement of all necessary parameters to comprehensively assess  
677 the photosynthetic apparatus in leaves. This approach enables a holistic understanding of how  
678 photosynthesis is optimized. A primer on measuring photorespiration is given as Supplementary  
679 File S1.

680

### 681 *Natural genetic variation in photosynthetic parameters as a basis for breeding*

682

683 One way to adapt plants to human requirements is by harnessing the natural genetic variation  
684 that has been generated through random mutations over historical time spans. This genetic  
685 variation can occur at both, the intraspecific and the interspecific level.

686 The first evidence of natural genetic variation in the context of photorespiration was provided by  
687 Jorda and Ogren (1981). They observed differences in the specificity factors towards the  
688 substrates CO<sub>2</sub> and O<sub>2</sub>,  $S_{c/o}$ , of Rubiscos purified from seven different species, ranging from 77  
689 to 82. Subsequent studies, as reviewed by Hartmann and Harpel (1994), revealed changes in the  
690 specificity factor due to replacement of the active-site metal, random and site-directed  
691 mutagenesis, chemical modification, and hybridization of heterologous subunits. The highest  
692 reported specificity factor for Rubisco is 238, found in the red alga *Galdieria partita* (Uemura et

693 al., 1996), which is about three times higher than that reported for Rubisco from most crop plants  
694 (Parry et al., 1989).

695 Even before the discovery of the oxygenase activity of Rubisco (Bowes et al., 1971), selection  
696 experiments aiming to manipulate the specificity factor of Rubisco through selection were  
697 conducted (*cf.* Cannell et al., 1969; Menz et al., 1969). In these experiments, plants were kept at  
698 or slightly above the compensation point, and plants with high rates of photorespiration were  
699 expected to perish.

700 As discussed in the previous section, over the recent years, the number of studies exploring the  
701 natural plasticity and inherent variability of Rubisco's key catalytic traits has significantly  
702 increased. Information about the interspecific variation in photorespiration has also been  
703 observed through carbon isotope fractionation (Lanigan et al., 2008). However, to the best of our  
704 knowledge, only the study by Cai et al. (2014) examined and observed natural genetic variation  
705 in CO<sub>2</sub> compensation points and evaluated these differences in the context of leaf anatomy  
706 variations among three *Rhododendron* species.

707 The genes or alleles responsible for the advantageous photorespiratory phenotype can be  
708 transferred through interspecific hybridization, protoplast fusion, transformation, or genome  
709 editing. To facilitate these processes, it is necessary to identify the underlying genes or alleles.  
710 One approach to achieve this is through large-scale comparative genomics, which incorporates  
711 phenotypic information and is referred to as phylogenetic association mapping (*e.g.*, Collins and  
712 Didelot, 2018).

713 However, with the exception of Schlüter et al. (2023), no earlier study has considered natural  
714 variation in characters related to photorespiration in a densely sampled phylogenetic tree, making  
715 the application of phylogenetic association mapping challenging for identifying the underlying  
716 genomic features.

717 An alternative approach for identifying the genomic features responsible for interspecific  
718 differences is the utilization of segregating genetic material derived from interspecific hybrids.

719 Comparative transcriptomics is another approach that can aid in identifying the *cis* and *trans*  
720 factors responsible for interspecific differences. By comparing transcriptomes of accessions  
721 adapted to specific conditions or subjected to environmental perturbations, strategies for crop  
722 improvement can be guided. For example, in rice, RNA sequencing identified a transcription factor  
723 with the potential to enhance photosynthetic capacity and increase yield (Wei et al., 2022).  
724 However, when using bulk RNA sequencing of an organ, it becomes challenging to detect  
725 differentially expressed genes specific to rare cell types, as their expression is diluted. In the case  
726 of C<sub>3</sub>-C<sub>4</sub> or C<sub>4</sub> photosynthesis, where the pathways operate in specific cell types of the leaf,

727 obtaining cell-type-specific transcriptomes is crucial. Approaches such as mechanical separation  
728 of cell types (John et al., 2014) and laser capture microdissection followed by microarray/RNAseq  
729 have been used previously, but their scale and resolution are limited by the speed of sampling,  
730 and separating low abundance cell types can still be challenging (Zhang et al., 2007; Aubry et al.,  
731 2014; Hua et al., 2021; Xiong et al., 2021).

732 The adoption of single-cell methods, particularly droplet-based technology, is gaining increasing  
733 acceptance in plant research. This approach allows the capture of individual transcriptomic  
734 profiles of cells from a wide range of plant species, providing valuable insights at a remarkably  
735 low cost per cell. For example, comparative single-cell analysis of roots from three grass species  
736 provided significant insights into the evolution of cellular divergence in these crops (Guillot et  
737 al., 2023). As such, this approach therefore must hold potential for better understanding the  
738 compartmentation of gene expression in  $C_3$ - $C_4$  and  $C_4$  species (Cuperus, 2021; Seyfferth et al.,  
739 2021). Currently the number of single-cell or single nuclei datasets generated from leaf tissues is  
740 limited and most studies have tended to focus on a single model species under one condition  
741 (Berrío et al., 2021; Bezruczyk et al., 2021; Kim et al., 2021; Lopez-Anido et al., 2021; Procko et  
742 al., 2022; Sun et al., 2022). To enhance photosynthetic efficacy in crops, understanding the  
743 changes in gene expression associated with closely related  $C_3$ ,  $C_4$  or/and  $C_3$ - $C_4$  intermediate  
744 species is likely to provide insights into the molecular signatures of each of these traits, and  
745 therefore how they might be rationally engineered. Comparative analysis of leaf anatomy, cellular  
746 ultrastructure and photosynthetic traits between species within a genus, for example in  
747 *Gynandropsis* (Marshall et al., 2007; Koteyeva et al., 2011), *Moricandia* (Schlüter et al., 2017), or  
748 *Flaveria* (McKown and Dengler, 2007; Kümpers et al., 2017) have provided insights into traits that  
749 engender higher photosynthesis efficiency. Therefore, acquiring transcriptome data from  
750 individual bundle sheath and mesophyll cells of these closely related plants should provide new  
751 insights into how the patterns of transcript abundance alter in association with modifications to  
752 photosynthetic efficiency. We also anticipate that single-cell RNAseq will contribute to crop  
753 improvement by providing insights into underlying molecular mechanisms. Lastly, additional  
754 advantages can be obtained from single-cell RNAseq if the data are associated with a complex  
755 phenotype (single-cell TWAS) and genotype (cell-type specific eQTL) at a population level (Perez  
756 et al., 2022). It seems likely that such approaches will be adopted for high resolution genotyping  
757 of bioengineered plants in synthetic biology projects. In summary, the combination of scRNAseq  
758 technology with comparative transcriptomics, population genetics, and synthetic biology is likely  
759 to serve as a powerful tool for crop improvement.

760 A technically simpler procedure to the above-described approach of exploiting interspecific natural  
761 genetic variation would be the exploitation of the intraspecific variation within the species under  
762 consideration for photosynthetic properties as the transfer or the enrichment of the positive alleles  
763 is much easier to realize in comparison to the interspecific variability. Within species, natural  
764 variation in leaf photosynthesis has been reported for model species (e.g., (Tomeo and  
765 Rosenthal, 2018) but also for major crops (e.g., Gu et al., 2012; Driever et al., 2014). However,  
766 the improvements that can be realized in that way are up to now smaller compared to the  
767 approaches exploiting interspecific variability.

768

### 769 **New-to-Nature Approaches to Improve Photosynthetic Efficiency**

770

771 Most efforts of improving carbon capture in plants have focused on engineering naturally existing  
772 enzymes and pathways (Kebeish et al., 2007; South et al., 2019). However, the emergence of  
773 synthetic biology has opened up the possibility to radically (re)draft plant metabolism to overcome  
774 the limitations of natural evolution, which is driven by co-linearity, tinkering, epistatic drift, and  
775 purifying selection, rather than by “design” (Wurtzel et al., 2019). Thus, such engineering  
776 approaches have the potential to expand the biological solution space and provide new-to-nature  
777 pathways that outcompete their natural counterparts in respect to thermodynamics and/or  
778 kinetics, because they are drafted from first principles.

779 As an example, while Nature has evolved seven different pathways for CO<sub>2</sub> fixation, more than  
780 30 synthetic CO<sub>2</sub> fixation pathways have already been designed, which are all superior to the  
781 CBC (Bar-Even et al., 2010). Some of these new-to-nature solutions have even been successfully  
782 realized *in vitro* (Schwander et al., 2016; Luo et al., 2022; McLean et al., 2023), and are awaiting  
783 their transplantation *in vivo*.

784 The concept of designer metabolism has also been extended to photorespiration lately (Figure  
785 3). Two studies have proposed alternative ways to use the photorespiratory metabolite glyoxylate  
786 to feed into synthetic carbon fixation cycles (Figure 3, pathways 1 & 2). The first cycle is the malyl-  
787 CoA-glycerate pathway (MCG). In this cycle, the bacterial glyoxylate assimilation route condenses  
788 two molecules of glyoxylate to form a C<sub>3</sub> compound, releasing CO<sub>2</sub> in the process. The resulting  
789 tartronate semialdehyde is then reduced and phosphorylated into 2-phosphoglycerate (2PG).  
790 2PG is converted to phosphoenolpyruvate and further carboxylated to oxaloacetate, subsequently  
791 reduced to malate and activated with coenzyme A, followed by cleavage into glyoxylate and  
792 acetyl-CoA. Glyoxylate is then available to initiate the next cycle, while acetyl-CoA can be utilized

793 for biosynthesis (Yu et al., 2018). The MGC pathway, therefore, does not result in a net loss of  
794 CO<sub>2</sub>.

795  
796 A second study proposed the 3-hydroxypropionate (3OHP) photorespiratory bypass, inspired by  
797 the naturally occurring 3OHP bi-cycle (Zarzycki et al., 2009). The 3OHP bypass exploits the malyl-  
798 CoA lyase to produce β-methylmalyl-CoA from glyoxylate and propionyl-CoA. Methylmalyl-CoA  
799 undergoes a series of interconversion that yield citramalyl-CoA, which in turn serves as a substrate  
800 for the malyl-CoA lyase and produces pyruvate and acetyl-CoA. Acetyl-CoA is carboxylated to  
801 malonyl-CoA, which is then reduced and further activated into the starter compound of the cycle:  
802 propionyl-CoA. Pyruvate on the other hand can be further converted to phosphoglycerate and re-  
803 enter the CBC (Shih et al., 2014) and resulting in a net gain in carbon.

804 Both studies implemented their proposed cycles in cyanobacteria. Regardless of the CO<sub>2</sub> fixing  
805 ability of 3OHP bypass, strains carrying the cycle did not present a conclusive phenotype.  
806 However, the authors set an example for the future *in vivo* implementation of carbon capturing  
807 photorespiratory bypasses. On the other hand, strains containing the MCG pathway showed  
808 increased bicarbonate assimilation, acetyl-CoA accumulation, and achieved higher optical  
809 densities than strains lacking MCG.

810 The aforementioned cycles, represent what has been described in literature as “mix and match”  
811 synthetic pathways, as they described novel pathways, relying on known reactions and enzymes  
812 (Erb et al., 2017). Nevertheless, a recent study has identified several new-to-nature pathways by  
813 systematically developing reaction sequences from the pool of feasible biochemical  
814 transformations that could convert (phospho)glycolate back into a central intermediate of the CBC  
815 cycle (Trudeau et al., 2018). The design of these solutions was guided by two additional principles.  
816 First, the new reaction sequences should require as little energy as possible, and second, these  
817 pathways should be CO<sub>2</sub>-neutral (i.e., do not release CO<sub>2</sub>) or even capture CO<sub>2</sub>.

818 Through these efforts, the authors proposed four “carbon neutral pathways” in order to  
819 reincorporate the C2 compound product of the oxygenation reaction of Rubisco into the CBC  
820 (Figure 3, pathways 3-6). These pathways rely on a novel reduction of glycolate to glycolaldehyde  
821 via engineered enzymes. Taking advantage of the high reactivity of glycolaldehyde, it is further  
822 combined with sugar phosphates present on the CBC such as: Glyceraldehyde 3-phosphate  
823 (GAP), dihydroxyacetone phosphate (DHAP), fructose 6-phosphate or sedoheptulose 7-  
824 phosphate (S7P) via aldolase, transketolase or transaldolase reactions. In all cases, a C5  
825 compound is produced and further converted into the substrate of rubisco, ribulose 1,5-  
826 biphosphate. In the case of the transketolase and transaldolase reactions side products are

827 formed that are also part of the CBC and therefore, can directly be reused. Trudeau et al. proved  
828 the *in vitro* feasibility of one of their proposed carbon neutral bypasses, however, to-date no further  
829 improvement or *in vivo* implementation has been reported (Trudeau et al., 2018).

830 Furthermore, in the same study, another photorespiration bypass comprising novel reactions was  
831 proposed, the tartronyl-CoA (TaCo) pathway (Figure 3, pathway 7). The TaCo pathway is a five-  
832 reaction sequence that first converts photorespiratory glycolate into glycolyl-CoA, which is  
833 subsequently carboxylated into tartronyl-CoA, the namesake compound of the pathway. In two  
834 subsequent steps, tartronyl-CoA is then reduced to glycerate, which can re-enter the CBB cycle  
835 at the level of phosphoglycerate. Compared to natural photorespiration, the TaCo pathway  
836 sequence is about 50% shorter, requires about 20% less ATP and 30% less reducing power,  
837 does not release ammonia, and notably also not CO<sub>2</sub>, but instead captures additional CO<sub>2</sub> during  
838 photorespiration. In other words, through the TaCo pathway, photorespiration can be turned into  
839 a carbon-capturing process, in which the oxygenation reaction of Rubisco will still lead to a fixation  
840 of carbon subsequently.

841 Although this pathway outcompetes natural photorespiration, a challenge has been that the  
842 central TaCo pathway sequence relies on enzyme reactions that have not been described, thus  
843 far. This apparent challenge was addressed through re-engineering the active sites of enzyme  
844 candidates that catalyze similar reactions to establish and/or improve the desired reactions  
845 (Scheffen et al., 2021). The full pathway was reconstituted and prototyped *in vitro*.

846 Yet, this proof-of-principle is only the starting point for further developments to successfully realize  
847 the TaCo pathway in the context of the living plant. This could be achieved through a combination  
848 of complementary approaches. The *in vitro* prototyping efforts could be expanded by combining  
849 high throughput combinatorics with machine learning guided experimentation to optimize the  
850 enzyme stoichiometry and robustness of the pathway (Pandi et al., 2022; Vögeli et al., 2022). The  
851 optimized network could then be (partially) transplanted in a suitable (micro)organism to test for  
852 its feasibility and use adaptive laboratory evolution (ALE) to further improve the network and its  
853 cellular integration. The latter strategy has been recently successfully used to establish the CBC,  
854 the reverse glycine cleavage pathway or a modified serine cycle in *E. coli* (Antonovsky et al.,  
855 2016; Yishai et al., 2017; Gleizer et al., 2019; Luo et al., 2022), in which selection strains were  
856 designed, which need to form (part) of their biomass through the new pathways. Having  
857 established a functional cycle inside of a microorganisms will guide further efforts to integrate this  
858 new reaction sequence in plants.

859

860

## 861 **Concluding Remarks and Perspectives**

862 Sustainably increasing crop yields is crucial to meet the growing demands of a rising global  
863 population for food, feed, and other plant-derived products. Maximizing photosynthetic efficiency  
864 is hence an important factor for food security in the context of anthropogenic climate change and  
865 resource limitations. In the quest for increasing crop productivity through improvement of  
866 photosynthetic efficiency, bypasses to canonical photorespiration and modifications of excess  
867 light protection have been designed, implemented in several model species and in crops and  
868 have been tested in the field. Jointly, these data provide proof-of-concept for yield increases  
869 through engineering of photorespiration and light harvesting.

870 While progress has been made, there are still unanswered questions that need to be addressed,  
871 essential to fully gather the potential improvements achievable from these approaches. For  
872 example, how do photorespiratory bypasses actually work? What are the mechanisms that  
873 underpin the observed yield increases? Resolving questions such as these will require additional  
874 experiments and comprehensive analysis by mathematical models of plant metabolism.

875 Available data suggest that combining photorespiratory bypasses with optimized energy  
876 dissipation holds promise for maximizing the energy available for CO<sub>2</sub> assimilation. New-to-nature  
877 pathways show potential to exceed the yield improvements that have been achieved by current  
878 photorespiratory bypasses. To date, these pathways have been prototyped *in vitro* and in  
879 bacteria, and they are awaiting testing in plants.

880 Furthermore, natural variation in photosynthetic efficiency exists in both domesticated crops and  
881 their wild relatives, and so provides a valuable resource for breeding strategies. Techniques such  
882 as intra- and inter-specific hybridization and genome editing could leverage promising alleles  
883 identified through pan-genomic association mapping and systems biology approaches to  
884 introduce beneficial genetic variants into crops. Knowledge of the natural variation in  
885 photosynthetic parameters should be combined with synthetic photorespiratory bypasses for  
886 synergistic effects. For example, alternative forms of Rubisco with higher  $V_c$  at the cost of lower  
887  $V_c/V_o$  could be combined with more energy efficient or CO<sub>2</sub> concentrating photorespiratory  
888 bypasses, resulting in additive benefits. Also, it should be possible to combine more performant  
889 Rubisco variants with better sourcing of CO<sub>2</sub> via optimization of  $g_m$ . The CO<sub>2</sub> compensation point  
890 serves as a key parameter in screening for photosynthetic efficiency; multiple methods have been  
891 employed for its determination, but its precision relies on accurate estimation of cellular CO<sub>2</sub>  
892 effluxes and influxes.

893 The efficacy of increasing photosynthetic efficiency in crops in the field has been clearly  
894 demonstrated, but further improvements, or reliable transfer of traits from model organisms to

895 crop species, or between crop species, will likely require additional modifications of sink tissues  
896 or harvestable biomass to reap the full benefits of increased photosynthetic efficiency. Only if sink  
897 strength can keep up with source capacity it will be possible to capitalize on gains in efficiency.  
898 The practicality of implementing different strategies for improving photosynthetic efficiency that  
899 range from selective breeding to new-to-nature pathways depends on government regulation of  
900 genetic modification, which must be also considered when applying scientific discoveries to solve  
901 real world problems.

902

903

#### 904 **Acknowledgements**

905 We appreciate funding by the European Union H2020 Program (project GAIN4CROPS, GA No.  
906 862087, to BS, GF, TM, TE, APMW, MH, OE, JMH, and TT) and the Deutsche  
907 Forschungsgemeinschaft (Cluster of Excellence for Plant Sciences (CEPLAS) under Germany's  
908 Excellence Strategy EXC-2048/1 under project ID 390686111 to BS, OE and APMW; CRC TRR  
909 341 "Plant Ecological Genetics" to BS and APMW).

910

#### 911 **Supplementary Materials**

912

913 Supplementary Text S1: A primer on measuring photorespiration

914

915 Supplementary Table 1: Energy budget accounting for photorespiratory bypasses

916

917



918 **References**

- 919
- 920
- 921 **Abadie, C., and Tcherkez, G.** (2019). Plant sulphur metabolism is stimulated by  
922 photorespiration. *Commun. Biology* **2**: 379.
- 923 **Abbasi, A. Z., Bilal, M., Khurshid, G., Yiotis, C., Zeb, I., Hussain, J., Baig, A., Shah, M. M.,**  
924 **Chaudhary, S. U., Osborne, B., et al.** (2021). Expression of cyanobacterial genes  
925 enhanced CO<sub>2</sub> assimilation and biomass production in transgenic *Arabidopsis thaliana*. *Peer*  
926 *J.* **9**: e11860.
- 927 **Alboresi, A., Storti, M., and Morosinotto, T.** (2019). Balancing protection and efficiency in the  
928 regulation of photosynthetic electron transport across plant evolution. *New Phytol.* **221**: 105–  
929 109.
- 930 **Antonovsky, N., Gleizer, S., Noor, E., Zohar, Y., Herz, E., Barenholz, U., Zelcbuch, L.,**  
931 **Amram, S., Wides, A., Tepper, N., et al.** (2016). Sugar Synthesis from CO<sub>2</sub> in *Escherichia*  
932 *coli*. *Cell* **166**: 115–125.
- 933 **Aubry, S., Kelly, S., Kümpers, B. M. C., Smith-Unna, R. D., and Hibberd, J. M.** (2014). Deep  
934 Evolutionary Comparison of Gene Expression Identifies Parallel Recruitment of Trans-  
935 Factors in Two Independent Origins of C<sub>4</sub> Photosynthesis. *PLoS Genet.* **10**: e1004365.
- 936 **Bar-Even, A., Noor, E., Lewis, N. E., and Milo, R.** (2010). Design and analysis of synthetic  
937 carbon fixation pathways. *Proc. Natl. Acad. Sci. U S A* **107**: 8889–8894.
- 938 **Basler, G., Küken, A., Fernie, A. R., and Nikoloski, Z.** (2016). Photorespiratory Bypasses  
939 Lead to Increased Growth in *Arabidopsis thaliana*: Are Predictions Consistent with  
940 Experimental Evidence? *Frontiers Bioeng. Biotechnol.* **4**: 31.
- 941 **Bauwe, H.** (2023). Photorespiration – Rubisco’s repair crew. *J. Plant Physiol.* **280**:153899.
- 942 **Bauwe, H., Hagemann, M., and Fernie, A. R.** (2010). Photorespiration: players, partners and  
943 origin. *Trends Plant Sci.* **15**: 330–336.
- 944 **Bernacchi, C. J., Bagley, J. E., Serbin, S. P., Ruiz-Vera, U. M., Rosenthal, D. M., and**  
945 **Vanloocke, A.** (2013). Modelling C<sub>3</sub> photosynthesis from the chloroplast to the ecosystem.  
946 *Plant Cell Environ.* **36**: 1641–1657.
- 947 **Berrío, R. T., Verstaen, K., Vandamme, N., Pevernagie, J., Achon, I., Duyse, J. V.,**  
948 **Isterdael, G. V., Saeys, Y., Veylder, L. D., Inzé, D., et al.** (2022). Single-cell transcriptomics  
949 sheds light on the identity and metabolism of developing leaf cells. *Plant Physiol.* **188**: 898–  
950 918.
- 951 **Bezruczyk, M., Zöllner, N. R., Kruse, C. P. S., Hartwig, T., Lautwein, T., Köhrer, K.,**  
952 **Frommer, W. B., and Kim, J.-Y.** (2021). Evidence for phloem loading via the abaxial bundle  
953 sheath cells in maize leaves. *Plant Cell* **33**: 531–547.
- 954 **Bilal, M., Abbasi, A. Z., Khurshid, G., Yiotis, C., Hussain, J., Shah, M. M., Naqvi, T., Kwon,**  
955 **S.-Y., Park, Y.-I., Osborne, B., et al.** (2019). The expression of cyanobacterial glycolate–  
956 decarboxylation pathway genes improves biomass accumulation in *Arabidopsis thaliana*.  
957 *Plant Biotechnol. Rep.* **13**: 361–373.
- 958 **Bouvier, J. W., Emms, D. M., Rhodes, T., Bolton, J. S., Brasnett, A., Eddershaw, A.,**  
959 **Nielsen, J. R., Unitt, A., Whitney, S. M., and Kelly, S.** (2021). Rubisco Adaptation Is More  
960 Limited by Phylogenetic Constraint Than by Catalytic Trade-off. *Mol. Biol. Evol.* **38**: 2880–  
961 2896.

- 962 **Bowes, G., Ogren, W. L., and Hageman, R. H.** (1971). Phosphoglycolate production catalyzed  
963 by ribulose diphosphate carboxylase. *Biochem. Biophys. Res. Commun.* **45**: 716–722.
- 964 **Broncano, L. S., Pukacz, K. R., Reichel-Deland, V., Schlüter, U., Triesch, S., and Weber, A.**  
965 **P. M.** (2023). Photorespiration is the solution, not the problem. *J Plant Physiol.* **282**: 153928.
- 966 **Busch, F. A.** (2020). Photorespiration in the context of Rubisco biochemistry, CO<sub>2</sub> diffusion and  
967 metabolism. *Plant J.* **101**: 919–939.
- 968 **Busch, F. A., Sage, T. L., Cousins, A. B., and Sage, R. F.** (2013). C<sub>3</sub> plants enhance rates of  
969 photosynthesis by reassimilating photorespired and respired CO<sub>2</sub>. *Plant Cell Environ.* **36**:  
970 200–212.
- 971 **Cai, Y.-F., Li, S.-F., Li, S.-F., Xie, W.-J., and Song, J.** (2014). How do leaf anatomies and  
972 photosynthesis of three Rhododendron species relate to their natural environments? *Bot.*  
973 *Stud.* **55**: 36.
- 974 **Campbell, W. J., and Ogren, W. L.** (1990). A novel role for light in the activation of  
975 ribulosebiphosphate carboxylase/oxygenase. *Plant Physiol.* **92**: 110–5.
- 976 **Cannell, R. Q., Brun, W. A., and Moss, D. N.** (1969). A Search for High Net Photosynthetic  
977 Rate among Soybean Genotypes1. *Crop Sci.* **9**: 840–841.
- 978 **Carvalho, J. de F. C., Madgwick, P. J., Powers, S. J., Keys, A. J., Lea, P., and Parry, M. A.**  
979 **J.** (2011). An engineered pathway for glyoxylate metabolism in tobacco plants aimed to  
980 avoid the release of ammonia in photorespiration. *BMC Biotechnol.* **11**: 111.
- 981 **Clarke, V. C., Rosa, A. D., Massey, B., George, A. M., Evans, J. R., Caemmerer, S. von, and**  
982 **Groszmann, M.** (2022). Mesophyll conductance is unaffected by expression of Arabidopsis  
983 PIP1 aquaporins in the plasmalemma of Nicotiana. *J. Exp. Bot.* **73**: 3625–3636.
- 984 **Collins, C., and Didelot, X.** (2018). A phylogenetic method to perform genome-wide  
985 association studies in microbes that accounts for population structure and recombination.  
986 *PLoS Comput. Biol.* **14**: e1005958.
- 987 **Cuperus, J. T.** (2021). Single-cell genomics in plants: current state, future directions, and  
988 hurdles to overcome. *Plant Physiol.* **188**: 749–755.
- 989 **Cutolo, E. A., Guardini, Z., Dall’Osto, L., and Bassi, R.** (2023). A paler shade of green:  
990 engineering cellular chlorophyll content to enhance photosynthesis in crowded environments.  
991 *New Phytol.* Advance Access published 2023, doi:10.1111/nph.19064.
- 992 **Dalal, J., Lopez, H., Vasani, N. B., Hu, Z., Swift, J. E., Yalamanchili, R., Dvora, M., Lin, X.,**  
993 **Xie, D., Qu, R., et al.** (2015). A photorespiratory bypass increases plant growth and seed  
994 yield in biofuel crop *Camelina sativa*. *Biotechnol. Biofuels* **8**: 175.
- 995 **Driever, S. M., Lawson, T., Andralojc, P. J., Raines, C. A., and Parry, M. A. J.** (2014).  
996 Natural variation in photosynthetic capacity, growth, and yield in 64 field-grown wheat  
997 genotypes. *J. Exp. Bot.* **65**:4959–4973.
- 998 **Eisenhut, M., Ruth, W., Haimovich, M., Bauwe, H., Kaplan, A., and Hagemann, M.** (2008).  
999 The photorespiratory glycolate metabolism is essential for cyanobacteria and might have  
1000 been conveyed endosymbiontically to plants. *Proc. Natl. Acad. Sci. U S A* **105**: 17199–  
1001 17204.
- 1002 **Eisenhut, M., Roell, M., and Weber, A. P. M.** (2019). Mechanistic understanding of  
1003 photorespiration paves the way to a new green revolution. *New Phytol.* **223**: 1762–1769.

- 1004 **Erb, T. J., Jones, P. R., and Bar-Even, A.** (2017). Synthetic metabolism: metabolic  
1005 engineering meets enzyme design. *Curr. Opin. Chem. Biol.* **37**: 56–62.
- 1006 **Evans, J. R.** (2021). Mesophyll conductance: walls, membranes and spatial complexity. *New*  
1007 *Phytol.* **229**: 1864–1876.
- 1008 **Fernie, A. R., and Bauwe, H.** (2020). Wasteful, essential, evolutionary stepping stone? The  
1009 multiple personalities of the photorespiratory pathway. *Plant J.* **102**: 666–677.
- 1010 **Flexas, J., Barbour, M. M., Brendel, O., Cabrera, H. M., Carriquí, M., Díaz-Espejo, A.,**  
1011 **Douthe, C., Dreyer, E., Ferrio, J. P., Gago, J., et al.** (2012). Mesophyll diffusion  
1012 conductance to CO<sub>2</sub>: An unappreciated central player in photosynthesis. *Plant Sci.* **193**: 70–  
1013 84.
- 1014 **Flexas, J., Niinemets, U., Gallé, A., Barbour, M. M., Centritto, M., Díaz-Espejo, A., Douthe,**  
1015 **C., Galmés, J., Ribas-Carbo, M., Rodriguez, P. L., et al.** (2013). Diffusional conductances  
1016 to CO<sub>2</sub> as a target for increasing photosynthesis and photosynthetic water-use efficiency.  
1017 *Photosynth. Res.* **117**: 45–59.
- 1018 **Flexas, J., and Carriquí, M.** (2020). Photosynthesis and photosynthetic efficiencies along the  
1019 terrestrial plant's phylogeny: lessons for improving crop photosynthesis. *Plant J.* **101**: 964–  
1020 978.
- 1021 **Flügel, F., Timm, S., Arrivault, S., Florian, A., Stitt, M., Fernie, A. R., and Bauwe, H.** (2017).  
1022 The Photorespiratory Metabolite 2-Phosphoglycolate Regulates Photosynthesis and Starch  
1023 Accumulation in Arabidopsis. *Plant Cell* **29**: 2537–2551.
- 1024 **Fu, X., Gregory, L. M., Weise, S. E., and Walker, B. J.** (2023a). Integrated flux and pool size  
1025 analysis in plant central metabolism reveals unique roles of glycine and serine during  
1026 photorespiration. *Nat. Plants* **9**: 169–178.
- 1027 **Fu, X., Smith, K., Gregory, L., Roze, L., and Walker, B.** (2023b). Understanding and  
1028 improving crop photosynthesis. *Burleigh Dodds Ser. Agric. Sci.* Advance Access published  
1029 2023, doi:10.19103/as.2022.0119.12.
- 1030 **Gago, J., Carriquí, M., Nadal, M., Clemente-Moreno, M. J., Coopman, R. E., Fernie, A. R.,**  
1031 **and Flexas, J.** (2019). Photosynthesis Optimized across Land Plant Phylogeny. *Trends*  
1032 *Plant Sci.* **24**: 947–958.
- 1033 **Galmés, J., Capó-Bauçà, S., Niinemets, Ü., and Iñiguez, C.** (2019). Potential improvement of  
1034 photosynthetic CO<sub>2</sub> assimilation in crops by exploiting the natural variation in the temperature  
1035 response of Rubisco catalytic traits. *Curr. Opin. Plant Biol.* **49**: 60–67.
- 1036 **Garcia-Molina, A., and Leister, D.** (2020). Accelerated relaxation of photoprotection impairs  
1037 biomass accumulation in Arabidopsis. *Nat. Plants* **6**: 9–12.
- 1038 **Gleizer, S., Ben-Nissan, R., Bar-On, Y. M., Antonovsky, N., Noor, E., Zohar, Y., Jona, G.,**  
1039 **Krieger, E., Shamshoum, M., Bar-Even, A., et al.** (2019). Conversion of *Escherichia coli* to  
1040 Generate All Biomass Carbon from CO<sub>2</sub>. *Cell* **179**: 1255-1263.e12.
- 1041 **Gu, J., Yin, X., Stomph, T.-J., Wang, H., and Struik, P. C.** (2012). Physiological basis of  
1042 genetic variation in leaf photosynthesis among rice (*Oryza sativa* L.) introgression lines  
1043 under drought and well-watered conditions. *J. Exp. Bot.* **63**: 5137–5153.

- 1044 **Guillotin, B., Rahni, R., Passalacqua, M., Mohammed, M. A., Xu, X., Raju, S. K., Ramírez,**  
1045 **C. O., Jackson, D., Groen, S. C., Gillis, J., et al. (2023).** A pan-grass transcriptome reveals  
1046 patterns of cellular divergence in crops. *Nature* **617**: 785–791.
- 1047 **Hanawa, H., Ishizaki, K., Nohira, K., Takagi, D., Shimakawa, G., Sejima, T., Shaku, K.-I.,**  
1048 **Makino, A., and Miyake, C. (2017).** Land plants drive photorespiration as higher electron-  
1049 sink: Comparative study of post-illumination transient O<sub>2</sub>-uptake rates from liverworts to  
1050 angiosperms through ferns and gymnosperms. *Physiol. Plantarum* **161(1)**: 138-149.
- 1051 **Hartman, F. C., and Harpel, M. R. (1994).** Structure, Function, Regulation, and Assembly of D-  
1052 Ribulose-1,5-Bisphosphate Carboxylase/Oxygenase. *Annu. Rev. Biochem.* **63**: 197–232.
- 1053 **Heber, U., and Krause, G. H. (1980).** What is the physiological role of photorespiration? *Trends*  
1054 *Biochem. Sci.* **5**: 32–34.
- 1055 **Heber, U., Bligny, R., Streb, P., and Douce, R. (1996).** Photorespiration is Essential for the  
1056 Protection of the Photosynthetic Apparatus of C<sub>3</sub> Plants Against Photoinactivation Under  
1057 Sunlight. *Bot. Acta* **109**: 307–315.
- 1058 **Hodges, M., Dellerio, Y., Keech, O., Betti, M., Raghavendra, A. S., Sage, R., Zhu, X.-G.,**  
1059 **Allen, D. K., and Weber, A. P. M. (2016).** Perspectives for a better understanding of the  
1060 metabolic integration of photorespiration within a complex plant primary metabolism network.  
1061 *J. Exp. Bot.* **67**: 3015–3026.
- 1062 **Hua, L., Stevenson, S. R., Reyna-Llorens, I., Xiong, H., Kopriva, S., and Hibberd, J. M.**  
1063 **(2021).** The bundle sheath of rice is conditioned to play an active role in water transport as  
1064 well as sulfur assimilation and jasmonic acid synthesis. *Plant J.* **107**: 268–286.
- 1065 **Iqbal, W. A., Lisitsa, A., and Kapralov, M. V. (2023).** Predicting plant Rubisco kinetics from  
1066 RbcL sequence data using machine learning. *J. Exp. Bot.* **74**: 638–650.
- 1067 **John, C. R., Smith-Unna, R. D., Woodfield, H., Covshoff, S., and Hibberd, J. M. (2014).**  
1068 Evolutionary Convergence of Cell-Specific Gene Expression in Independent Lineages of C<sub>4</sub>  
1069 Grasses. *Plant Physiol.* **165**: 62–75.
- 1070 **Jordan, D. B., and Ogren, W. L. (1981).** Species variation in the specificity of ribulose  
1071 biphosphate carboxylase/oxygenase. *Nature* **291**: 513–515.
- 1072 **Kebeish, R., Niessen, M., Thiruveedhi, K., Bari, R., Hirsch, H.-J., Rosenkranz, R., Stähler,**  
1073 **N., Schönfeld, B., Kreuzaler, F., and Peterhänsel, C. (2007).** Chloroplastic  
1074 photorespiratory bypass increases photosynthesis and biomass production in *Arabidopsis*  
1075 *thaliana*. *Nat. Biotechnol.* **25**: 593–599.
- 1076 **Khurshid, G., Abbassi, A. Z., Khalid, M. F., Gondal, M. N., Naqvi, T. A., Shah, M. M.,**  
1077 **Chaudhary, S. U., and Ahmad, R. (2020).** A cyanobacterial photorespiratory bypass model  
1078 to enhance photosynthesis by rerouting photorespiratory pathway in C<sub>3</sub> plants. *Sci. Rep.* **10**:  
1079 20879.
- 1080 **Kim, J.-Y., Symeonidi, E., Pang, T. Y., Denyer, T., Weidauer, D., Bezruczyk, M., Miras, M.,**  
1081 **Zöllner, N., Hartwig, T., Wudick, M. M., et al. (2021).** Distinct identities of leaf phloem cells  
1082 revealed by single cell transcriptomics. *Plant Cell* **33**: 511–530.
- 1083 **Knauer, J., Zaehle, S., Kauwe, M. G. D., Haverd, V., Reichstein, M., and Sun, Y. (2020).**  
1084 Mesophyll conductance in land surface models: effects on photosynthesis and transpiration.  
1085 *Plant J.* **101**: 858–873.

- 1086 Knauer, J., Cuntz, M., Evans, J. R., Niinemets, Ü., Tosens, T., Veromann-Jürgenson, L.-L.,  
1087 Werner, C., and Zaehle, S. (2022). Contrasting anatomical and biochemical controls on  
1088 mesophyll conductance across plant functional types. *New Phytol.* **236**: 357–368.
- 1089 Koteyeva, N. K., Voznesenskaya, E. V., Roalson, E. H., and Edwards, G. E. (2011). Diversity  
1090 in forms of C<sub>4</sub> in the genus *Cleome* (Cleomaceae). *Ann. Bot.* **107**: 269–283.
- 1091 Kozaki, A., and Takeba, G. (1996). Photorespiration protects C<sub>3</sub> plants from photooxidation.  
1092 *Nature* **384**: 557–560.
- 1093 Kromdijk, J., and McCormick, A. J. (2022). Genetic variation in photosynthesis: many variants  
1094 make light work. *J. Exp. Bot.* **73**: 3053–3056.
- 1095 Kromdijk, J., Głowacka, K., Leonelli, L., Gabilly, S. T., Iwai, M., Niyogi, K. K., and Long, S.  
1096 P. (2016). Improving photosynthesis and crop productivity by accelerating recovery from  
1097 photoprotection. *Science* **354**: 857–861.
- 1098 Kümpers, B. M. C., Burgess, S. J., Reyna-Llorens, I., Smith-Unna, R., Bournnell, C., and  
1099 Hibberd, J. M. (2017). Shared characteristics underpinning C<sub>4</sub> leaf maturation derived from  
1100 analysis of multiple C<sub>3</sub> and C<sub>4</sub> species of *Flaveria*. *J. Exp. Bot.* **68**: 177–189.
- 1101 Laisk, A., Oja, V., Rasulov, B., Rämna, H., Eichelmann, H., Kasparova, I., Pettai, H., Padu,  
1102 E., and Vapaavuori, E. (2002). A computer-operated routine of gas exchange and optical  
1103 measurements to diagnose photosynthetic apparatus in leaves: Diagnosing photosynthesis.  
1104 *Plant Cell Environ.* **25**: 923–943.
- 1105 Lanigan, G. J., Betson, N., Griffiths, H., and Seibt, U. (2008). Carbon Isotope Fractionation  
1106 during Photorespiration and Carboxylation in *Senecio*. *Plant Physiol.* **148**: 2013–2020.
- 1107 Levey, M., Timm, S., Mettler-Altmann, T., Borghi, G. L., Koczor, M., Arrivault, S., Weber, A.  
1108 P., Bauwe, H., Gowik, U., and Westhoff, P. (2019). Efficient 2-phosphoglycolate  
1109 degradation is required to maintain carbon assimilation and allocation in the C<sub>4</sub> plant *Flaveria*  
1110 *bidentis*. *J. Exp. Bot.* **70**: 575–587.
- 1111 Li, Z., Wakao, S., Fischer, B. B., and Niyogi, K. K. (2009). Sensing and Responding to  
1112 Excess Light. *Annu. Rev. Plant Biol.* **60**: 239–260.
- 1113 Long, S. P., Taylor, S. H., Burgess, S. J., Carmo-Silva, E., Lawson, T., Souza, A. P. D.,  
1114 Leonelli, L., and Wang, Y. (2022). Into the Shadows and Back into Sunlight: Photosynthesis  
1115 in Fluctuating Light. *Annu. Rev. Plant Biol.* **73**: 617–648.
- 1116 Lopez-Anido, C. B., Vatén, A., Smoot, N. K., Sharma, N., Guo, V., Gong, Y., Gil, M. X. A.,  
1117 Weimer, A. K., and Bergmann, D. C. (2021). Single-cell resolution of lineage trajectories in  
1118 the *Arabidopsis* stomatal lineage and developing leaf. *Dev. Cell* **56**: 1043-1055.e4.
- 1119 Luo, S., Lin, P. P., Nieh, L.-Y., Liao, G.-B., Tang, P.-W., Chen, C., and Liao, J. C. (2022). A  
1120 cell-free self-replenishing CO<sub>2</sub>-fixing system. *Nat. Catal.* **5**: 154–162.
- 1121 Maier, A., Fahnenstich, H., Caemmerer, S. von, Engqvist, M. K. M., Weber, A. P. M.,  
1122 Flügge, U.-I., and Maurino, V. G. (2012). Transgenic Introduction of a Glycolate Oxidative  
1123 Cycle into *A. thaliana* Chloroplasts Leads to Growth Improvement. *Front Plant Sci.* **3**: 38.
- 1124 Marshall, D. M., Muhaidat, R., Brown, N. J., Liu, Z., Stanley, S., Griffiths, H., Sage, R. F.,  
1125 and Hibberd, J. M. (2007). *Cleome*, a genus closely related to *Arabidopsis*, contains species  
1126 spanning a developmental progression from C<sub>3</sub> to C<sub>4</sub> photosynthesis. *Plant J.* **51**: 886–896.
- 1127 McKown, A. D., and Dengler, N. G. (2007). Key innovations in the evolution of Kranz anatomy  
1128 and C<sub>4</sub> vein pattern in *Flaveria* (Asteraceae). *Am. J. Bot.* **94**: 382–399.

- 1129 **McLean, R., Schwander, T., Diehl, C., Cortina, N. S., Paczia, N., Zarzycki, J., and Erb, T. J.**  
1130 (2023). Exploring alternative pathways for the in vitro establishment of the HOPAC cycle for  
1131 synthetic CO<sub>2</sub> fixation. *Sci. Adv.* **9**: eadh4299.
- 1132 **Menz, K. M., Moss, D. N., Cannell, R. Q., and Brun, W. A.** (1969). Screening for  
1133 Photosynthetic Efficiency<sup>1</sup>. *Crop Sci.* **9**: 692–694.
- 1134 **Niinemets, Ü.** (2023). Variation in leaf photosynthetic capacity within plant canopies:  
1135 optimization, structural and physiological constraints and inefficiencies. *Photosynthesis Res.*  
1136 Advance Access published 2023.
- 1137 **Nobel, P. S.** (1991). Achievable productivities of certain CAM plants: basis for high values  
1138 compared with C<sub>3</sub> and C<sub>4</sub> plants. *New Phytol.* **119**: 183–205.
- 1139 **Nölke, G., Houdelet, M., Kreuzaler, F., Peterhansel, C., and Schillberg, S.** (2014). The  
1140 expression of a recombinant glycolate dehydrogenase polyprotein in potato (*Solanum*  
1141 *tuberosum*) plastids strongly enhances photosynthesis and tuber yield. *Plant Biotechnol. J.*  
1142 **12**: 734–742.
- 1143 **Oliver, D. J.** (1980). The effect of glyoxylate on photosynthesis and photorespiration by isolated  
1144 soybean mesophyll cells. *Plant Physiol.* **65**: 888–892.
- 1145 **Oliver, D. J., and Zelitch, I.** (1977). Increasing photosynthesis by inhibiting photorespiration  
1146 with glyoxylate. *Science* **196**: 1450–1451.
- 1147 **Onoda, Y., Wright, I. J., Evans, J. R., Hikosaka, K., Kitajima, K., Niinemets, Ü., Poorter, H.,**  
1148 **Tosens, T., and Westoby, M.** (2017). Physiological and structural tradeoffs underlying the  
1149 leaf economics spectrum. *New Phytol.* **214**: 1447–1463.
- 1150 **Osmanoglu, Ö., AlSeiari, M. K., AlKhoori, H. A., Shams, S., Bencurova, E., Dandekar, T.,**  
1151 **and Naseem, M.** (2021). Topological Analysis of the Carbon-Concentrating CETCH Cycle  
1152 and a Photorespiratory Bypass Reveals Boosted CO<sub>2</sub>-Sequestration by Plants. *Front.*  
1153 *Bioeng. Biotechnol.* **9**: 708417.
- 1154 **Pandi, A., Diehl, C., Kharrazi, A. Y., Scholz, S. A., Bobkova, E., Faure, L., Nattermann, M.,**  
1155 **Adam, D., Chapin, N., Foughijabbari, Y., et al.** (2022). A versatile active learning  
1156 workflow for optimization of genetic and metabolic networks. *Nat. Commun.* **13**: 3876.
- 1157 **Parry, M. A. J., Keys, A. J., and Gutteridge, S.** (1989). Variation in the Specificity Factor of C<sub>3</sub>  
1158 Higher Plant Rubiscos Determined by the Total Consumption of Ribulose-P 2. *J. Exp. Bot.*  
1159 **40**: 317–320.
- 1160 **Perez, R. K., Gordon, M. G., Subramaniam, M., Kim, M. C., Hartoularos, G. C., Targ, S.,**  
1161 **Sun, Y., Ogorodnikov, A., Bueno, R., Lu, A., et al.** (2022). Single-cell RNA-seq reveals cell  
1162 type-specific molecular and genetic associations to lupus. *Science* **376**: eabf1970.
- 1163 **Perin, G., Bellan, A., Michelberger, T., Lyska, D., Wakao, S., Niyogi, K. K., and**  
1164 **Morosinotto, T.** (2023). Modulation of xanthophyll cycle impacts biomass productivity in the  
1165 marine microalga *Nannochloropsis*. *Proc. Natl. Acad. Sci. U S A* **120**: e2214119120.
- 1166 **Peterhansel, C., Blume, C., and Offermann, S.** (2013). Photorespiratory bypasses: how can  
1167 they work? *J. Exp. Bot.* **64**: 709–715.
- 1168 **Pick, T. R., Bräutigam, A., Schulz, M. A., Obata, T., Fernie, A. R., and Weber, A. P. M.**  
1169 (2013). PLGG1, a plastidic glycolate glycerate transporter, is required for photorespiration

- 1170 and defines a unique class of metabolite transporters. *Proc National Acad Sci U S A* **110**:  
1171 3185–3190.
- 1172 **Procko, C., Lee, T., Borsuk, A., Bargmann, B. O. R., Dabi, T., Nery, J. R., Estelle, M., Baird,**  
1173 **L., O'Connor, C., Brodersen, C., et al.** (2022). Leaf cell-specific and single-cell  
1174 transcriptional profiling reveals a role for the palisade layer in UV light protection. *Plant Cell*  
1175 **34**: 3261–3279.
- 1176 **Roell, M.-S., Borzyskowski, L. S. von, Westhoff, P., Plett, A., Paczia, N., Claus, P.,**  
1177 **Schlueter, U., Erb, T. J., and Weber, A. P. M.** (2021). A synthetic C<sub>4</sub> shuttle via the β-  
1178 hydroxyaspartate cycle in C<sub>3</sub> plants. *Proc National Acad Sci U S A* **118**: e2022307118.
- 1179 **Rotasperti, L., Tadini, L., Chiara, M., Crosatti, C., Guerra, D., Tagliani, A., Forlani, S.,**  
1180 **Ezquer, I., Horner, D. S., Jahns, P., et al.** (2022). The barley mutant *happy under the sun 1*  
1181 (*hus1*): An additional contribution to pale green crops. *Environ. Exp. Bot.* **196**: 104795.
- 1182 **Saadat, N. P., Nies, T., Aalst, M. van, Hank, B., Demirtas, B., Ebenhöf, O., and**  
1183 **Matuszyńska, A.** (2021). Computational Analysis of Alternative Photosynthetic Electron  
1184 Flows Linked With Oxidative Stress. *Front. Plant Sci.* **12**: 750580.
- 1185 **Sage, R. F.** (2002). Variation in the  $k_{cat}$  of Rubisco in C<sub>3</sub> and C<sub>4</sub> plants and some implications for  
1186 photosynthetic performance at high and low temperature. *J. Exp. Bot.* **53**: 609–620.
- 1187 **Samuilov, S., Brillhaus, D., Rademacher, N., Flachbart, S., Arab, L., Alfarraj, S., Kuhnert,**  
1188 **F., Kopriva, S., Weber, A. P. M., Mettler-Altmann, T., et al.** (2018). The Photorespiratory  
1189 BOU Gene Mutation Alters Sulfur Assimilation and Its Crosstalk With Carbon and Nitrogen  
1190 Metabolism in *Arabidopsis thaliana*. *Front Plant Sci* **9**: 1709.
- 1191 **Scheffen, M., Marchal, D. G., Beneyton, T., Schuller, S. K., Klose, M., Diehl, C., Lehmann,**  
1192 **J., Pfister, P., Carrillo, M., He, H., et al.** (2021). A new-to-nature carboxylation module to  
1193 improve natural and synthetic CO<sub>2</sub> fixation. *Nat Catal* **4**: 105–115
- 1194 **Schlüter, U., Bräutigam, A., Gowik, U., Melzer, M., Christin, P.-A., Kurz, S., Mettler-**  
1195 **Altmann, T., and Weber, A. P.** (2017). Photosynthesis in C<sub>3</sub>–C<sub>4</sub> intermediate *Moricandia*  
1196 species. *J. Exp. Bot.* **68**: 191–206.
- 1197 **Schlüter, U., Bouvier, J. W., Guerreiro, R., Malisic, M., Kontny, C., Westhoff, P., Stich, B.,**  
1198 **and Weber, A. P. M.** (2023). Brassicaceae display diverse photorespiratory carbon  
1199 recapturing mechanisms. *J Exp Bot: erad250*. doi: 10.1093/jxb/erad250
- 1200 **Schwander, T., Borzyskowski, L. S. von, Burgener, S., Cortina, N. S., and Erb, T. J.** (2016).  
1201 A synthetic pathway for the fixation of carbon dioxide in vitro. *Science* **354**: 900–904.
- 1202 **Seyfferth, C., Renema, J., Wendrich, J. R., Eekhout, T., Seurinck, R., Vandamme, N., Blob,**  
1203 **B., Saeys, Y., Helariutta, Y., Birnbaum, K. D., et al.** (2021). Advances and Opportunities of  
1204 Single-Cell Transcriptomics for Plant Research. *Annu. Rev. Plant Biol.* **72**: 1–20.
- 1205 **Shen, B.-R., Wang, L.-M., Lin, X.-L., Yao, Z., Xu, H.-W., Zhu, C.-H., Teng, H.-Y., Cui, L.-L.,**  
1206 **Liu, E. E., Zhang, J.-J., et al.** (2019). Engineering a New Chloroplastic Photorespiratory  
1207 Bypass to Increase Photosynthetic Efficiency and Productivity in Rice. *Mol. Plant* **12**: 199–  
1208 214.
- 1209 **Shih, P. M., Zarzycki, J., Niyogi, K. K., and Kerfeld, C. A.** (2014). Introduction of a synthetic  
1210 CO<sub>2</sub>-fixing photorespiratory bypass into a cyanobacterium. *J. Biol. Chem.* **289**: 9493–9500.
- 1211 **South, P. F., Cavanagh, A. P., Liu, H. W., and Ort, D. R.** (2019). Synthetic glycolate  
1212 metabolism pathways stimulate crop growth and productivity in the field. *Science* **363**:  
1213 eaat9077.

- 1214 **Souza, A. P. D., Burgess, S. J., Doran, L., Hansen, J., Manukyan, L., Maryn, N., Gotarkar,**  
1215 **D., Leonelli, L., Niyogi, K. K., and Long, S. P.** (2022). Soybean photosynthesis and crop  
1216 yield are improved by accelerating recovery from photoprotection. *Science* **377**: 851–854.
- 1217 **Sun, G., Xia, M., Li, J., Ma, W., Li, Q., Xie, J., Bai, S., Fang, S., Sun, T., Feng, X., et al.**  
1218 (2022). The maize single-nucleus transcriptome comprehensively describes signaling  
1219 networks governing movement and development of grass stomata. *Plant Cell* **34**: 1890–  
1220 1911.
- 1221 **Tcherkez, G., and Farquhar, G. D.** (2021). Rubisco catalytic adaptation is mostly driven by  
1222 photosynthetic conditions – Not by phylogenetic constraints. *J. Plant Physiol.* **267**: 153554.
- 1223 **Timm, S., Woitschach, F., Heise, C., Hagemann, M., and Bauwe, H.** (2019). Faster Removal  
1224 of 2-Phosphoglycolate through Photorespiration Improves Abiotic Stress Tolerance of  
1225 *Arabidopsis*. *Plants Basel Switz* **8**: 563.
- 1226 **Tomeo, N. J., and Rosenthal, D. M.** (2018). Photorespiration differs among *Arabidopsis*  
1227 *thaliana* ecotypes and is correlated with photosynthesis. *J. Exp. Bot.* **69**: 5191–5204.
- 1228 **Tosens, T., Niinemets, Ü., Westoby, M., and Wright, I. J.** (2012). Anatomical basis of  
1229 variation in mesophyll resistance in eastern Australian sclerophylls: news of a long and  
1230 winding path. *J. Exp. Bot.* **63**: 5105–5119.
- 1231 **Trudeau, D. L., Edlich-Muth, C., Zarzycki, J., Scheffen, M., Goldsmith, M., Khersonsky, O.,**  
1232 **Avizemer, Z., Fleishman, S. J., Cotton, C. A. R., Erb, T. J., et al.** (2018). Design and in  
1233 vitro realization of carbon-conserving photorespiration. *Proc National Acad Sci U S A* **115**:  
1234 E11455–E11464.
- 1235 **Uemura, K., Suzuki, Y., Shikanai, T., Wadano, A., Jensen, R. G., Chmara, W., and Yokota,**  
1236 **A.** (1996). A Rapid and Sensitive Method for Determination of Relative Specificity of  
1237 RuBisCO from Various Species by Anion-Exchange Chromatography. *Plant Cell Physiol.* **37**:  
1238 325–331.
- 1239 **Vögeli, B., Schulz, L., Garg, S., Tarasava, K., Clomburg, J. M., Lee, S. H., Gonnot, A.,**  
1240 **Mouilly, E. H., Kimmel, B. R., Tran, L., et al.** (2022). Cell-free prototyping enables  
1241 implementation of optimized reverse  $\beta$ -oxidation pathways in heterotrophic and autotrophic  
1242 bacteria. *Nat. Commun.* **13**: 3058.
- 1243 **Walker, B. J., Vanloocke, A., Bernacchi, C. J., and Ort, D. R.** (2016a). The Costs of  
1244 Photorespiration to Food Production Now and in the Future. *Annu. Rev. Plant Biol.* **67**: 107–  
1245 129.
- 1246 **Walker, B. J., Skabelund, D. C., Busch, F. A., and Ort, D. R.** (2016b). An improved approach  
1247 for measuring the impact of multiple CO<sub>2</sub> conductances on the apparent photorespiratory  
1248 CO<sub>2</sub> compensation point through slope–intercept regression. *Plant Cell Environ.* **39**: 1198–  
1249 1203.
- 1250 **Wang, L.-M., Shen, B.-R., Li, B.-D., Zhang, C.-L., Lin, M., Tong, P.-P., Cui, L.-L., Zhang, Z.-**  
1251 **S., and Peng, X.-X.** (2020a). A Synthetic Photorespiratory Shortcut Enhances  
1252 Photosynthesis to Boost Biomass and Grain Yield in Rice. *Mol. Plant* **13**: 1802–1815.
- 1253 **Walker, B. J., Drewry, D. T., Slattery, R. A., VanLoocke, A., Cho, Y. B., and Ort, D. R.**  
1254 (2017). Chlorophyll Can Be Reduced in Crop Canopies with Little Penalty to Photosynthesis.  
1255 *Plant Physiol.* **176**: 1215–1232.



- 1256 **Wang, X., Wang, Y., Ling, A., Guo, Z., Asim, M., Song, F., Wang, Q., Sun, Y., Khan, R., Yan,**  
1257 **H., et al.** (2020b). Rationale: Photosynthesis of Vascular Plants in Dim Light. *Front. Plant*  
1258 *Sci.* **11**: 573881.
- 1259 **Wei, S., Li, X., Lu, Z., Zhang, H., Ye, X., Zhou, Y., Li, J., Yan, Y., Pei, H., Duan, F., et al.**  
1260 (2022). A transcriptional regulator that boosts grain yields and shortens the growth duration  
1261 of rice. *Science* **377**: eabi8455.
- 1262 **Wu, A.** (2023). Modelling plants across scales of biological organisation for guiding crop  
1263 improvement. *Funct. Plant Biol.* **50**: 435–454.
- 1264 **Wurtzel, E. T., Vickers, C. E., Hanson, A. D., Millar, A. H., Cooper, M., Voss-Fels, K. P.,**  
1265 **Nikel, P. I., and Erb, T. J.** (2019). Revolutionizing agriculture with synthetic biology. *Nat.*  
1266 *Plants* **5**: 1207–1210.
- 1267 **Xin, C.-P., Tholen, D., Devloo, V., and Zhu, X.-G.** (2015). The benefits of photorespiratory  
1268 bypasses: how can they work? *Plant Physiol.* **167**: 574–585.
- 1269 **Xiong, H., Hua, L., Reyna-Llorens, I., Shi, Y., Chen, K.-M., Smirnov, N., Kromdijk, J., and**  
1270 **Hibberd, J. M.** (2021). Photosynthesis-independent production of reactive oxygen species in  
1271 the rice bundle sheath during high light is mediated by NADPH oxidase. *Proc. Natl. Acad.*  
1272 *Sci. U S A* **118**: e2022702118.
- 1273 **Yishai, O., Goldbach, L., Tenenboim, H., Lindner, S. N., and Bar-Even, A.** (2017).  
1274 Engineered Assimilation of Exogenous and Endogenous Formate in *Escherichia coli*. *ACS*  
1275 *Synth. Biol.* **6**: 1722–1731.
- 1276 **Yu, H., Li, X., Duchoud, F., Chuang, D. S., and Liao, J. C.** (2018). Augmenting the Calvin-  
1277 Benson-Bassham cycle by a synthetic malyl-CoA-glycerate carbon fixation pathway. *Nat*  
1278 *Commun* **9**: 2008.
- 1279 **Zarzycki, J., Brecht, V., Müller, M., and Fuchs, G.** (2009). Identifying the missing steps of the  
1280 autotrophic 3-hydroxypropionate CO<sub>2</sub> fixation cycle in *Chloroflexus aurantiacus*. *Proc.*  
1281 *National Acad. Sci. U S A* **106**: 21317–21322.
- 1282 **Zelitch, I., Schultes, N. P., Peterson, R. B., Brown, P., and Brutnell, T. P.** (2009). High  
1283 glycolate oxidase activity is required for survival of maize in normal air. *Plant Physiol.* **149**:  
1284 195–204.
- 1285 **Zhang, X., Madi, S., Borsuk, L., Nettleton, D., Elshire, R. J., Buckner, B., Janick-Buckner,**  
1286 **D., Beck, J., Timmermans, M., Schnable, P. S., et al.** (2007). Laser Microdissection of  
1287 Narrow Sheath Mutant Maize Uncovers Novel Gene Expression in the Shoot Apical  
1288 Meristem. *PLoS Genet.* **3**: e101.
- 1289 **Zhang, Z., Lu, Y., Zhai, L., Deng, R., Jiang, J., Li, Y., He, Z., and Peng, X.** (2012). Glycolate  
1290 Oxidase Isozymes Are Coordinately Controlled by GLO1 and GLO4 in Rice. *PLoS ONE* **7**:  
1291 e39658.
- 1292 **Zhang, C., Zhong, X., Lin, D., Wu, K., Wu, Z., Zhang, Z., and Peng, X.** (2022). Grain Quality  
1293 Affected by Introducing Photorespiratory Bypasses into Rice. *Agronomy* **12**: 566.
- 1294 **Zhu, X.-G., Long, S. P., and Ort, D. R.** (2010). Improving photosynthetic efficiency for greater  
1295 yield. *Annu. Rev. Plant Biol.* **61**: 235–261.
- 1296

1297 **Figure Legends**

1298

1299 **Figure 1.** Bypasses to photorespiration discussed in this review. 1) Wild type photorespiration; 2)  
 1300 Maier et al., 2012; 3) South et al., 2019; 4) Kebeish et al., 2007; 5) Shen et al., 2019; 6) Carvalho  
 1301 et al., 2011; 7) Roell et al., 2021.

1302

1303 **Figure 2.** Semi- and ultrathin cross-sections of *Helianthus occidentalis* leaf mesophyll (A) and  
 1304 palisade cells (B) to illustrate the CO<sub>2</sub> diffusion pathway from ambient air ( $C_a$ ) to substomatal  
 1305 cavities ( $C_i$ ); through intercellular airspaces to the outer surface of mesophyll cell wall ( $C_{i,w}$ ) and  
 1306 further into the chloroplast ( $C_c$ ). The CO<sub>2</sub> concentration drawdown,  $C_a - C_i$ , is modulated by  
 1307 stomatal conductance. Mesophyll conductance ( $g_m$ ) is determined by both gas- and liquid-phase  
 1308 conductance. The  $C_i - C_{i,w}$  drop is modulated by gas phase diffusion conductance ( $g_{ias}$ ),  
 1309 depending on mesophyll thickness and effective porosity of mesophyll airspace. The CO<sub>2</sub>  
 1310 drawdown from outer surface of cell walls to chloroplasts,  $C_{i,w} - C_c$ , is determined by liquid-phase  
 1311 diffusion conductance ( $g_{liq}$ ) that is determined by multiple liquid and lipid phase barriers: cell wall  
 1312 (cw), plasma membrane (pm), cytoplasm (cyt), chloroplast envelope (env), and chloroplast stroma  
 1313 (chl). Thus, the physical dimensions of each anatomical component of  $g_m$  determine its partial  
 1314 conductance, largely setting the maximum  $g_m$  in a given species (Tosens et al., 2012). In this  
 1315 context, the cell periphery facing the intercellular airspace (IAS) is largely enveloped by  
 1316 chloroplasts ( $S_c/S_{mes} \sim 1$ , b). On a global scale,  $S_c/S_{mes}$  varies from 0.3 to 0.98. A high  $S_c/S_{mes}$   
 1317 signifies the direct passage of CO<sub>2</sub> fluxes from the IAS into the chloroplasts, while, this  
 1318 configuration also facilitates the efficient recycling of respiratory CO<sub>2</sub> fluxes as chloroplasts are  
 1319 covered by mitochondria (M) (Busch et al., 2013). Scale bars: (A) 0.03 mm, (B) 2  $\mu$ m. Unpublished  
 1320 images by Tiina Tosens.

1321

1322 **Figure 3. Designed (new-to-nature) photorespiratory bypasses.** 1) Malyl-CoA-glycerate  
 1323 pathway (MCG) (Yu et al., 2018); 2) 3-hydroxypropionate bypass (3OHP) (Shih et al., 2014); 3),  
 1324 4), 5) & 6) carbon neutral bypasses (Trudeau et al., 2018); 7) tartronyl-CoA pathway (TaCo)  
 1325 (Scheffen et al., 2021).

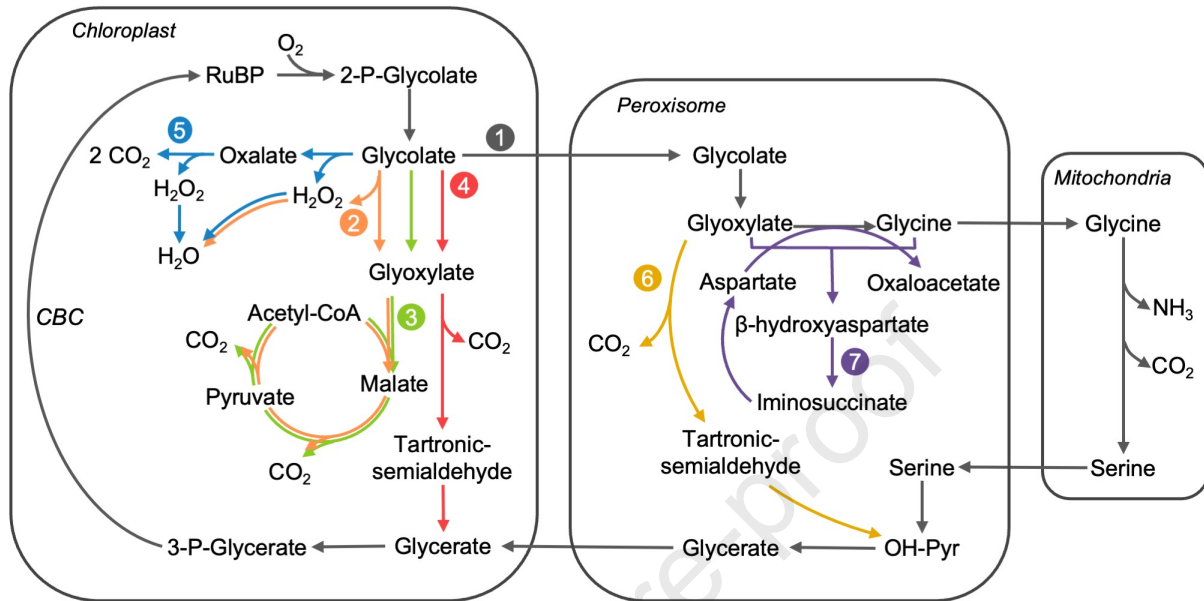
1326

1327

1328

1329

1330



Journal Pre-proof

